A SINGLE ELECTRON TUNNELING FORCE SPECTROSCOPY STUDY OF DIELECTRIC MATERIALS

by

Dustin W. Winslow

A dissertation submitted to the faculty of
The University of Utah
in partial fulfillment of the requirements for the degree of

Doctor of Philosophy

in

Physics

Department of Physics and Astronomy

The University of Utah

May 2012

The University of Utah Graduate School

STATEMENT OF DISSERTATION APPROVAL

The dissertation of **Dustin W. Winslow**

has been approved by the following supervisory committee members:

Clayton Williams	, Chair	**March 12, 2012** Date Approved
Scott Anderson	, Member	**March 12, 2012** Date Approved
Christoph Boehme	, Member	**March 12, 2012** Date Approved
Eugene Mishchenko	, Member	**March 19, 2012** Date Approved
Michael Vershinin	, Member	**March 12, 2012** Date Approved

and by **David Kieda**, Chair of the Department of **Physics and Astronomy**

and by Charles A. Wight, Dean of The Graduate School.

ABSTRACT

Single electron tunneling force microscopy has been developed over the last decade as a tool to manipulate the occupation and probe the properties of trap states in completely non conducting materials. The technique has been advanced through the efforts of several generations of graduate students in the Clayton Williams research group. Previous graduate students have demonstrated that the single electron tunneling force microscopy technique can repeatably facilitate single electron tunneling between a metallic tip and an electron trap state in a completely non conducting, dielectric material. Also the single electron tunneling force spectroscopy technique has been shown to make these measurements with atomic scale resolution. As solid state device technology rushes toward higher power and increasingly smaller devices single electron tunneling force microscopy is uniquely positioned to identify the properties of trap states in dielectric materials with atomic scale resolution. The main thrust of this work has been concerned with demonstrating a repeatable spectroscopic method which can be used to reliably measure the energy of electron and hole traps due to defect states in dielectric materials. The single electron tunneling force spectroscopy technique was used to make spectroscopic measurements at several places on the surface of SiO_2, Si_3N_4 and HfO_2 films. The spectra measured were compared to known trap states in both the theoretical and experimental literature. The data show that the density of trap states is not spatially homogeneous, but varies from measurement to measurement. Most of the defect states identified by the single electron tunneling force spectroscopy technique correspond nicely with trap state energies found in either the experimental or theoretical literature. However, several states, not found in the literature, have also been identified by the scanning electron tunneling force spectroscopy technique. Additionally single electron tunneling force spectroscopy has provided evidence of irreversible and reversible tunneling events

with irreversible tunneling predominantly near the conduction and valence bands. A noted asymmetry in the amount of irreversible tunneling in favor of trap states near the valence band edge has also been identified. Finally a first demonstration of state creation and characterization by SETFS in SiO_2 is discussed.

CONTENTS

ABSTRACT . . . . . **iii**

LIST OF FIGURES . . . . . **vii**

ACKNOWLEDGEMENTS . . . . . **ix**

CHAPTERS

1. INTRODUCTION **1**

1.1 Motivation and Objectives 1
1.2 Force Modulated Atomic Force Microscopy 2
1.3 Tunneling Conditions 5
1.4 Single Electron Tunneling Force Microscopy 9
1.5 Dielectric Materials and the MOSFET 12
1.6 Electron and Hole Traps in Dielectric Materials 17
1.7 References 19

2. LOCALIZED DEFECT STATES IN SILICON DIOXIDE AND SILICON NITRIDE FILMS **21**

2.1 Local Apparent Density of Trap States in SiO_2 and Si_3N_4 Films Studied by Single Electron Tunneling Force Spectroscopy 21
2.1.1 Abstract 22
2.1.2 Introduction 22
2.1.3 Method 23
2.1.4 Results and Discussion 27
2.1.5 Conclusion 34
2.2 References 36

3. LOCALIZED DEFECT STATES IN HAFNIUM OXIDE FILMS **38**

3.1 Nanometer Scale Study of HfO_2 Trap States Using Single Electron Tunneling Force Spectroscopy 38
3.1.1 Abstract 39
3.1.2 Article 39
3.2 References 49

4. REVERSIBLE AND IRREVERSIBLE CHARGING OF HAFNIUM OXIDE FILMS 51

4.1 Abstract 51
4.2 Introduction 51
4.3 Method 52
4.4 Results and Discussion 56
4.5 Conclusion 63
4.6 References 64

5. CREATION OF DEFECT STATES IN SILICON DIOXIDE FILMS USING ELECTRON STIMULATED DESORPTION 65

5.1 Motivation and Objectives 65
5.2 ESD Methodology 66
5.3 Results and Discussion 70
5.4 Summary of ESD Results 76
5.5 References 77

APPENDIX: COMPARISON OF TIP-GAP-SAMPLE CAPACITANCE MODELS 79

LIST OF FIGURES

1.1 Very basic diagram of the AFM system. Note that the microscope is located in vacuum. 3

1.2 Model of the tip-vacuum gap-dielectric system. 7

1.3 Toy model demonstrating the energy requirements necessary for an electron to elastically tunnel from the tip through the vacuum gap and into the electron trap state in the dielectric film. 8

1.4 Schematic showing a very basic MOSFET device. 13

1.5 Energy diagram of the MOS structure of the MOSFET discussed in Figure 1.4. 14

1.6 Simplified energy diagram of the MOS portion of the MOSFET shown in Figure 1.4. 15

2.1 Illustration showing states in the band gap of the dielectric that satisfy the conditions for tunneling. 24

2.2 Diagram showing the applied voltages as a function of time. 26

2.3 Six representative plots (three above and three below mid-gap) of the local apparent density of trap states in the SiO_2 band gap. 28

2.4 Spatially averaged apparent density of states for SiO_2. 31

2.5 Six representative plots (three above and three below mid-gap) of the relative apparent density of trap states in the Si_3N_4 band gap. 32

2.6 Average apparent density of states for Si_3N_4. 35

3.1 States in the band gap that satisfy the conditions for tunneling. Circles indicate filled states. 41

3.2 Diagram showing the applied voltages as a function of time. 43

3.3 Representative plots of the apparent density of trap states within the band gap of HfO_2. 45

3.4 Apparent density of HfO_2 trap states averaged over 40 measurements locations. 47

4.1 Graphical representation of a single measurement cycle. 54

4.2 Graphical representation showing the tip-gap-sample system during the relaxation experiment. 55

4.3 A representation of a voltage array used to probe the relaxation of charge in HfO_2. 57
4.4 Surface potential measurements on HfO_2 above the middle of the band gap. 58
4.5 Surface potential measurements on HfO_2 below the middle of the band gap. 60
4.6 Description of possible pathway for mobile charge in HfO_2. 62
5.1 Three traces showing typical height curves showing the frequency shift steps indicative of single electron tunneling events. 69
5.2 Comparison of surface topography before and after the state creation attempt. 71
5.3 Line cuts taken horizontally across Figure 5.2a and 5.2b. 72
5.4 SETFM height scans taken on SiO_2 before (a) and after (b, c) a 21.5 V pulse applied 8 Å above the SiO_2 surface. 73
5.5 Two traces taken in two places after voltage pulses. 75
A.1 Diagram showing the two capacitor models being compared. 80

ACKNOWLEDGEMENTS

I would like to thank Clayton Williams for all of his assistance and guidance over the last several years, and for allowing me to work in his lab on interesting and challenging problems. Jon Paul Johnson trained me in the use of the atomic force microscope and other lab equipment, and was helpful in many discussions that allowed me to move my research forward. Also Adam Payne was instrumental in keeping the lab up and running during the final portion of my career as a graduate student.

Thank you to my parents who have always encouraged me to better myself, and been very supportive of me throughout my entire educational career. My friends, both old and new, who have given meaningful advice and helped me relax during down time. Finally, and most importantly, I would like to thank Michelle Hui who has been my constant companion over the last five years. She has been there through all of the ups and downs of graduate school and is indispensable to me.

CHAPTER 1

INTRODUCTION

1.1 Motivation and Objectives

In this introduction an overview of the SETFM technique will be discussed followed by a brief discussion on the physics and function of dielectric materials in electronic devices. This is followed by an overview on the nature of electron and hole traps in dielectric materials.

SiO_2 has been used for decades as the go to material for gate dielectrics in solid state electronic devices. Its success is in large part due to both its large band gap ($\tilde{}$ 9 eV) and the relatively low number of defect states in the thermally grown oxide. However the demand for ever decreasing device size has begun to show silicon dioxide's limitations as a gate dielectric. Several dielectrics have been proposed to replace SiO_2 as the standard gate dielectric. The characterization of these materials is of the utmost importance if the advancement of solid state electronics is to continue.

Single electron tunneling force microscopy (SETFM) has been developed over the last decade with an eye toward characterizing electronically isolated electron and hole trap states in completely nonconducting materials. Although SETFM measurements have been made on dielectric materials such as SiO_2 and HfO_2, which have demonstrated the efficacy of the SETFM technique, a thorough study of the trap state energies in these dielectric materials has not been undertaken using this technique. The objective of the research herein has been to demonstrate the ability of SETFM to accurately measure the energy of trap states in gate dielectrics by comparing the results of single electron tunneling force spectroscopy (SETFS) measurements to those of more traditional techniques. The intent is to show that SETFS can be used to accurately map the energy of trap states in the band gap of dielectric materials

with atomic scale resolution.

1.2 Force Modulated Atomic Force Microscopy

Scanning probe microscopes (SPM) use nonoptical methodologies to probe various aspects of a surface without the diffraction limitations of a traditional optical microscope. The scanning tunneling microscope (STM), one of the various prolific SPM methodologies, was first demonstrated by Binnig *et al.* in 1982.[1] STM probes the sample surface by measuring the current tunneled through the vacuum gap between the tip and sample. While STM has been used to image surface topography with atomic scale resolution[2] as well as probe the properties of defect states in dielectric materials[3] and quantum dots[4] there are several limitations inherent to the technique. The foremost is the necessity of a constant current that is typically greater than 1 pA to measure the tips interaction with the surface. This limits the STM's ability to probe trap states in nonconducting materials unless the sample is extremely thin, on the order of a few angstroms, or has a high density of defect states that will facilitate hopping of electrons through the sample to the substrate. This deficiency causes a problem if one wants to probe electronically isolated defect states in dielectric materials. To this end single electron tunneling force microscopy (SETFM) was developed based upon the atomic force microscope.

All of the single electron tunneling techniques developed over the last decade in the Williams research group are performed with an atomic force microscope (AFM), which is in an ultra high vacuum (UHV) environment ($\sim 10^{-9}$ Torr). Figure 1.1 shows the basic setup of the AFM used in the Williams lab. A tightly focused light is incident on the back of a reflective cantilever. The light is then reflected onto a split silicon detector, which detects the deflection of the cantilever due to the probe tip's interaction with the sample surface. To minimize the possibility of surface morphology changes and tip damage the AFM is used in noncontact mode, in which the cantilever is vibrated at its resonant frequency. The amount of frequency shift away from the cantilever's resonant frequency is used to measure the tip-sample

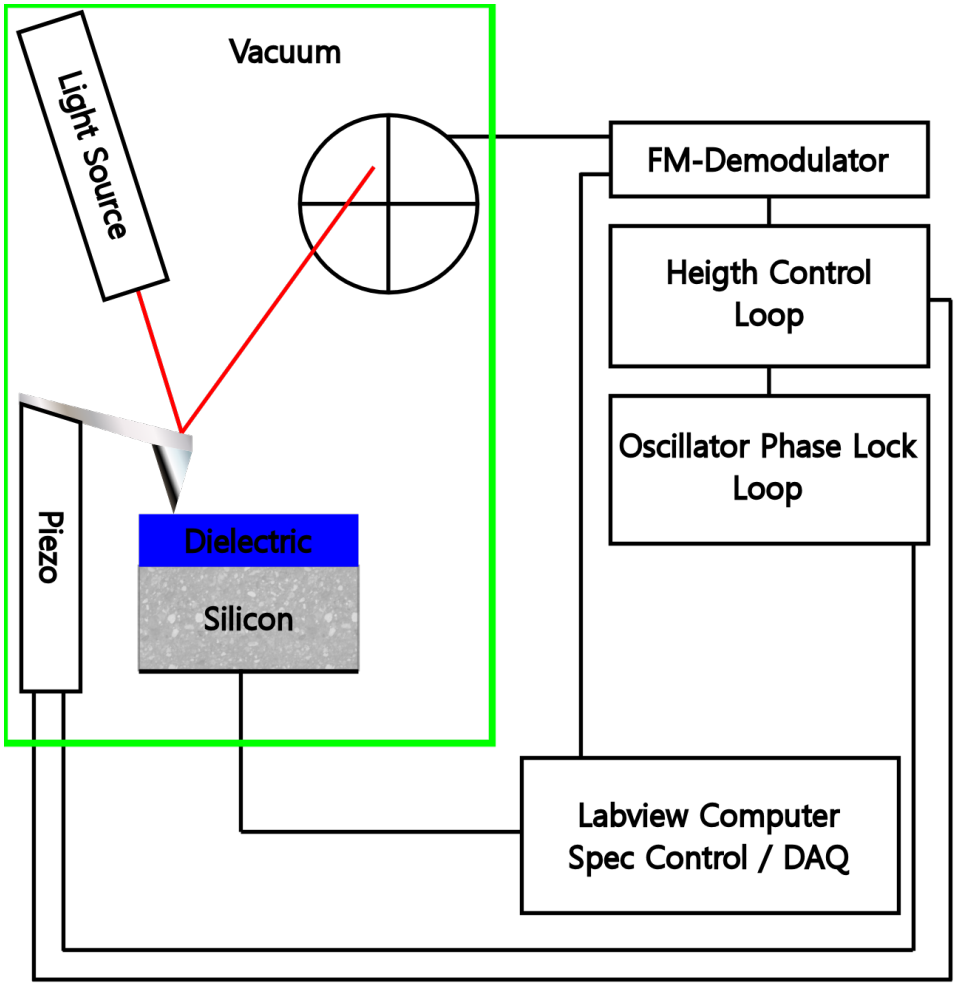

Figure 1.1: Very basic diagram of the AFM system. Note that the microscope is located in vacuum.

interaction. In order to model the oscillating cantilever it can be treated as a driven, damped harmonic oscillator governed by the equation[5, 6]

$$m^{\star}\ddot{z} + \frac{k}{Q\omega_0}\dot{z} + kz = F_d \tag{1.1}$$

where m_* is the effective mass of the cantilever, k is the spring constant of the cantilever, Q is the quality factor of the cantilever, ω_0 is the resonant frequency of the cantilever, F_d is the driving force required to keep the cantilever at its resonant frequency and z is the position of the free end of the cantilever in the direction of its oscillation. A driving force is controlled by an oscillator feedback loop that attempts to compensate the damping force and drive the oscillator at constant amplitude. When the cantilever is being oscillated on resonance the driving force will compensate for the damping of the cantilever (second term in equation 1.1), and the unperturbed equation of motion can then be rewritten as

$$m^{\star}\ddot{z} + kz = 0 \tag{1.2}$$

$$z = A\cos(\omega_0 t) \tag{1.3}$$

where A is the amplitude of the cantilever oscillation and t is the time.

When the cantilever is brought close to the surface it experiences a force, F, that is due to the electrostatic potential between the tip and the sample surface. Equations 1.2 and 1.3 can now be written as

$$m^{\star}\ddot{z} + kz = F \tag{1.4}$$

$$z = A\cos(\omega t) \tag{1.5}$$

where $\omega = \omega_0 + \Delta\omega$ is the new resonant frequency, which differs from the cantilever's natural resonant frequency by $\Delta\omega$. Plugging equation 1.5 into equation 1.4 gives

$$(\omega^2 - \omega_0^2)\cos(\omega t) = -\frac{\omega_0^2}{Ak}F \tag{1.6}$$

In the AFM being used the natural resonant frequency is on the order of 100 kHz and the frequency shift is on the order of 100 Hz ($\omega_0 \gg \Delta\omega$) so we can make the approximation $\omega^2 \cong \omega_0^2 + 2\omega_0\Delta\omega$ and can rewrite equation 1.6 as

$$2\Delta\omega\cos(\omega t) = -\frac{\omega_0}{Ak}F \tag{1.7}$$

Multiplying both sides of equation 1.7 by $\cos(\omega t)$, noting that F will vary as the cantilever oscillates and taking the time average of equation 1.7 gives

$$\langle\Delta\omega\rangle = -\frac{\omega_0}{Ak}\langle F\cos(\omega t)\rangle \tag{1.8}$$

Integrating over one oscillation cycle of the cantilever, and noting that the time average on the right hand side of the equation is calculated over an entire oscillation cycle and is insensitive to the substitution ω to ω_0, the shift in the cantilever's resonant frequency can be written as

$$\Delta f = -\frac{f_0}{\pi Ak}\int_{-1}^{+1}\frac{F(z_m + A(1+u))u}{\sqrt{1-u^2}}du \tag{1.9}$$

where z_m is the tip height at closest approach, A is the amplitude of cantilever oscillation, F is the interaction force between the tip and sample and $u = \cos(2\pi f_O t)$ is the substitution used to account for the oscillating tip position.[5, 6, 7] If a single electron tunnels between the tip and the sample surface the change in the force gradient will be apparent in the change in the resonant frequency of the cantilever.[8] For a more in depth discussion of frequency modulation atomic force microscopy and an example of how the frequency of the cantilever changes as a function of the voltage dropped between the tip and the sample see reference.[9]

1.3 Tunneling Conditions

Two conditions must be met, which will allow an electron to tunnel between the cantilever tip and the trap state in the dielectric. The first condition requires that the tunneling rate between the initial state in the tip and the final state in the sample be sufficiently fast so that the electron can tunnel during the measurement time. The second condition requires that the energy of the initial state in the tip must be

at the same energy as the occupied final state in the dielectric so that the electron can elastically tunnel from the tip to the dielectric state. The first condition will be discussed first.

An effective way to model the tunneling rate condition in the tip sample system can be seen in Figure 1.2. In the tip the electrons are in the Fermi sea of electrons below the Fermi level of the tip. In this model the state at the Fermi level of the tip can be approximated as a free electron state, while the trap state in the dielectric is localized and can be assumed to be a finite square well as can be seen in Figure 1.2. N. Zheng *et al.* modeled this tunneling condition and found that the tunneling rate from the tip to the sample trap state is strongly dependent on the tunneling gap between the tip and the sample. The tunneling rate falls off by an order of magnitude for each Å of increased gap distance.[10] Since the tunneling rate falls off so quickly only states directly under the tip will be available for tunneling. Nearby states, even as close as a few angstroms, will have a significantly lower tunneling rate. Therefore, by picking an appropriate tunneling gap the states directly under the tip can be made accessible to tunneling while nearby states are not available for tunneling.

The energy condition on the initial and final states is best understood from the toy model in Figure 1.3. For tunneling to take place the energy of the Fermi level of the metalized tip must be equal to or greater than the energy of the trap state in the dielectric medium. However it should be noted that the voltage applied to the sample with respect to the grounded tip is not the voltage used to determine the energy of trap states in the dielectric material. This is because some of the voltage is dropped in the vacuum gap and the rest is dropped across the dielectric film. Therefore, the applied voltage must be scaled to the voltage dropped between the tip and the state at the sample surface to determine the trap state energy. The voltage is scaled by using a parallel plate capacitor model to approximate the tip-sample system. Appendix A discusses a comparison between different models used to approximate the tip sample system. Also for a complete theoretical discussion of the tunneling model and the assumptions made see reference [10].

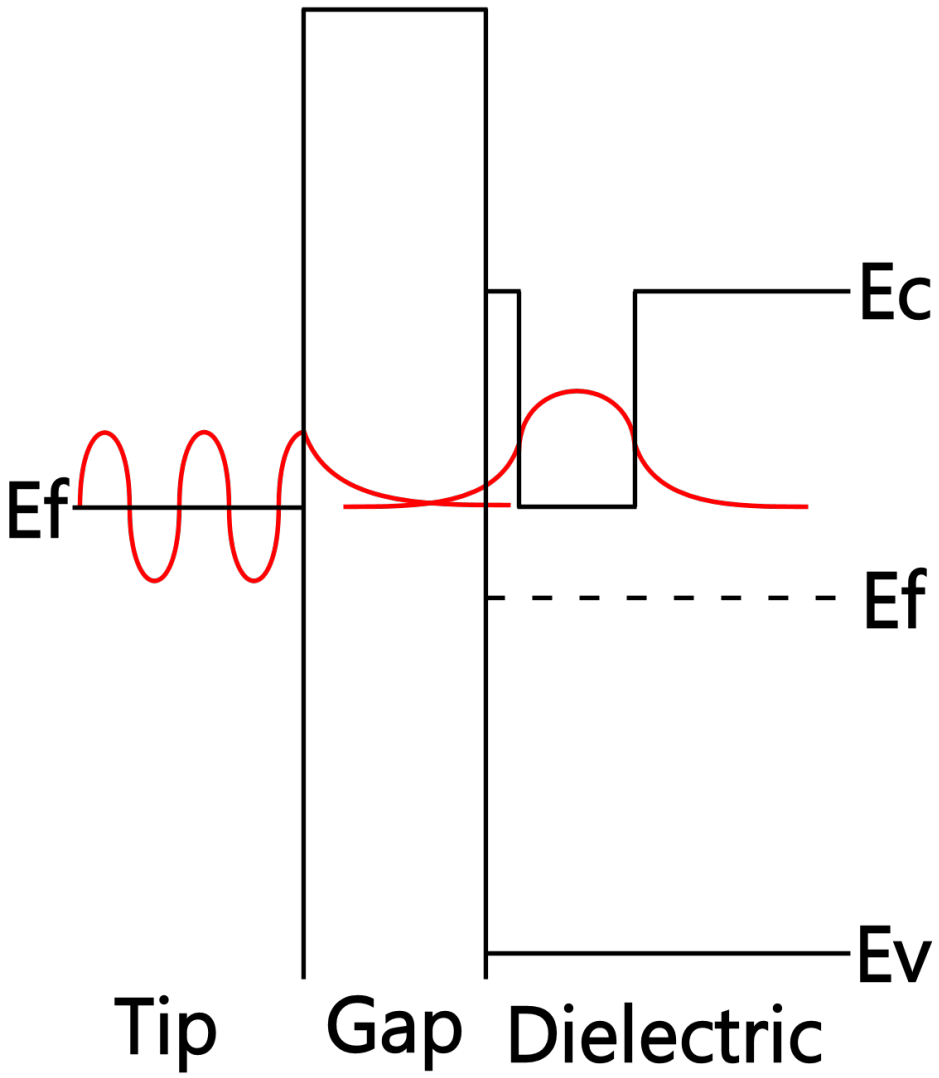

Figure 1.2: Model of the tip-vacuum gap-dielectric system. The trap state in the band gap is modeled as a finite well and the electron state in the tip is assumed to be a nearly free electron near the Fermi level of the tip. The tunneling rate from the tip to the trap state is dependent on the overlap of the two states.

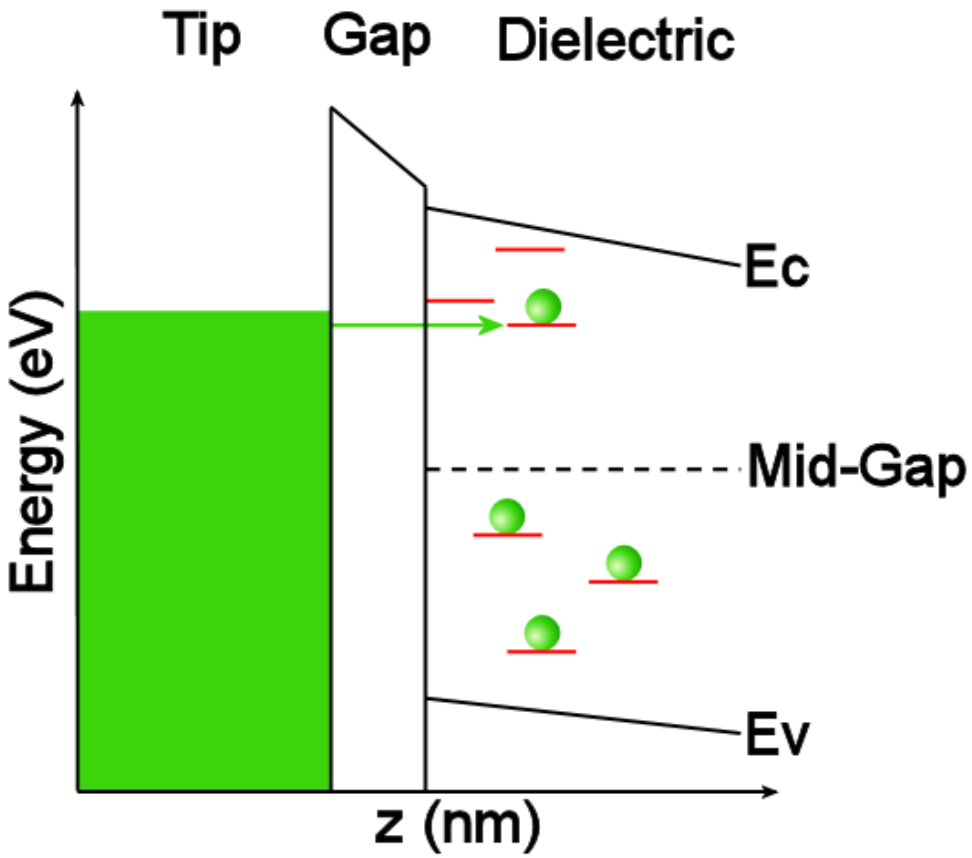

Figure 1.3: Toy model demonstrating the energy requirements necessary for an electron to elastically tunnel from the tip through the vacuum gap and into the electron trap state in the dielectric film. Note that an unfilled trap state in the dielectric is only filled if the Fermi level energy of the tip is at of higher than that of the trap state energy.

1.4 Single Electron Tunneling Force Microscopy

Over the last decade Single Electron Tunneling Force Microscopy (SETFM) has been improved and refined in order to establish a useful technique with the ability to characterize the properties of trap states in dielectric media. The first demonstration of single electron tunneling was made by Levi Klein *et al.* in which the ability to tunnel an electron from a metallic surface to a specially prepared scanning probe microscope tip demonstrated.[11] Later, Ezra Bussmann *et al.* demonstrated the detection of a single electron tunneling event from a metallic AFM probe to a localized trap state in SiO_2.[12] This improved demonstration of the SETFM technique allowed for characterization of unprepared, localized electron trap states in completely nonconducting materials. Tunneling of an electron is apparent as a step in the frequency shift of the cantilever as a function of tip height. While this technique provided evidence that electrons could tunnel to and from the sample surface its ability to quickly and accurately measure the energy of the trap state being probed was lacking. To this end further improvements in SETFM techniques were needed to establish the energy of electron trap states in the band gap of dielectric materials.

Scanning Electron Tunneling Force Spectroscopy (SETFS) was developed to fill the need to measure the energy of electron trap states in dielectric materials. The first form of the SETFS technique was applied by moving the tip within tunneling distance of the sample surface and varying the voltage between the tip and the sample.[13] In this technique the gap voltage at which the electron tunnels is equivalent to the energy (in eV) of the occupied state with respect to the middle of the dielectric band gap. Although the SETFS technique demonstrated by Bussmann *et al.* allowed the energy of the dielectric trap states to be measured there is a significant limitation inherent to this implementation of the SETFS technique. The drawback can be better understood after a short discussion of the physics that makes the measurement possible.

Earlier in the text it was shown that the frequency shift of the cantilever is dependent on the average force gradient acting on the cantilever tip. In this case the

force on the tip of the cantilever can be approximated as the force on the plate of the parallel plate capacitor and is given by

$$F(z) = -\frac{1}{2}\frac{\partial C}{\partial z}V^2 \tag{1.10}$$

where F(z) is the force on the cantilever as a function of the height z, C is the capacitance of the tip sample system which was described above and V is the voltage applied between the tip and the sample. Noting that the potential between the tip and the sample will depend on both the applied voltage used to scan through the band gap energy and the potential due to an electron that has tunneled to the surface from the tip (or from the surface to the tip) then the voltage (V) in equation 1.10 can be written as[12]

$$V = V_{App} \mp \frac{e}{C_{ox}} \cdot (\frac{t-d}{t}) \tag{1.11}$$

where V_{App} is the voltage applied between the tip and the sample, $C_{ox}$is the capacitance of the oxide layer of the film, d is the depth of the trap in the dielectric, t is the thickness of the dielectric and e is the elementary charge of the tunneled electron. The minus or plus sign indicates whether the surface charge is positive or negative. Plugging 1.11 into equation 1.10 and multiplying the squared term gives

$$F(z) \approxeq -\frac{1}{2}\frac{\partial C}{\partial z}(V_{App}^2 \mp 2\frac{e}{C_{ox}} \cdot (\frac{t-d}{t}) \cdot V_{App}) \tag{1.12}$$

where the $(\frac{e}{C_{ox}} \cdot (\frac{t-d}{t}))^2$ term has been dropped because $V_{App} \gg \frac{e}{C_{ox}} \cdot (\frac{t-d}{t})$ for the conditions under which the experiment is performed. As can be seen in equation 1.12 both terms in parentheses are dependent on the applied voltage. Unfortunately for applied voltages near 0 V the force on the cantilever becomes vanishingly small and detection of a tunneled electron becomes impossible. To eliminate the dependence of the frequency shift on the applied voltage a modification of the aforementioned spectroscopy technique is used.

Instead of simultaneously attempting to tunnel an electron between the tip and the sample and trying to detect evidence of a tunneled electron, a three-step methodology is used. First an AC square wave is applied to the sample, with respect to the

grounded tip, to measure the sample surface potential while the tip is out of tunneling range (~5 nm). The tip is then brought within tunneling range of the surface and an electron is tunneled to the surface by applying a DC voltage to the sample. Finally the surface potential is again measured by applying the AC square wave voltage to the sample while the tip is at a tip height outside of tunneling range of the sample (~5 nm). The difference between the surface potential measurements, made before and after the tunneling attempt, is proportional to the number of electrons that tunneled to the surface. During the surface potential measurement equation 1.10 will then take the form

$$F(z) = -\frac{1}{2}\frac{\partial C}{\partial z}(V_{SP} + V_{SQ}SQ(\omega t))^2 \tag{1.13}$$

where V_{SP} is the average surface potential difference between the tip and the sample, V_{SQ} is the magnitude of the square wave voltage with respect to the grounded tip, $SQ(\omega t)$ is a square wave that oscillates between +1 and -1 with frequency ω at time t. Taking the square then gives

$$F(z) = -\frac{1}{2}\frac{\partial C}{\partial z}(V_{SP}^2 + V_{SQ}^2 + 2V_{SP}V_{SQ}SQ(\omega t)) \tag{1.14}$$

In the time domain it is obvious that the squared square wave term contributes only a DC offset to the force acting on the cantilever. Using a lock-in amplifier centered on the frequency of the square wave the DC components are thrown out and the sensed force is now dependent only on the surface potential and the amplitude of the square wave. Using the surface potential methodology, in place of the one employed in reference [13], the tunneling of the electron has become decoupled from the sensing technique making the measurement sensitivity independent of the voltage used to tunnel. This surface potential measurement technique will be used to measure the energy of defect trap states in several materials used as gate dielectrics. These results will be compared to results from more traditional techniques that have been published in the literature.

1.5 Dielectric Materials and the MOSFET

A metal oxide semiconductor field effect transistor (MOSFET) is arguably the most important piece of technology in modern integrated circuits, and is also an ideal example when considering the limitations of SiO_2 as a gate dielectric. Figure 1.4 shows a general schematic for a basic MOSFET device. The device has three contacts; the source, the drain and the control gate. The source and drain contacts are laid down on top of a semiconducting region (n-type semiconductor in the case of Figure 1.4). Below the control gate contact is the gate oxide (gate dielectric) under which is the channel , which in the case of Figure 1.4 is a p-type doped semiconductor. The current, which flows from the source to the drain, is turned on and off by changing the voltage applied to the gate with respect to the drain. When no voltage is applied to the gate, the majority carriers (electrons) in the n-type region below the source are not able to flow through the channel (p-type region below the gate dielectric) to the drain. When a positive voltage is applied to the gate electrode the p-type dielectric is put into inversion, meaning that the minority carriers (electrons) in the p-type region are attracted toward the gate electrode. This inversion provides a path for the electrons to flow from the source to the drain.

The energy picture for the MOS structure in Figure 1.4 can be seen in Figure 1.5. The metal on the right represents the gate electrode, the oxide represents the gate dielectric and the p-type semiconductor represents the channel region of the semiconductor that has been doped to p-type. E_c is the conduction band of the oxide and semiconductor, E_i is the intrinsic Fermi level of the semiconductor, E_f is the Fermi level of the p-type doped semiconductor, E_v is the valence band of the semiconductor, d is the thickness of the gate dielectric, φ_m is the work function of the metal, χ and φ_s are the electron affinity and work function of the semiconductor, respectively, and $q\psi_B$ is the difference between the intrinsic Fermi level of the semiconductor and the doped Fermi level. A simplified version of the MOS energy diagram in Figure 1.6 shows qualitatively how an applied voltage on the gate electrode effects the charge carriers in the semiconducting film. Figure 1.6a shows an energy diagram of the metal oxide

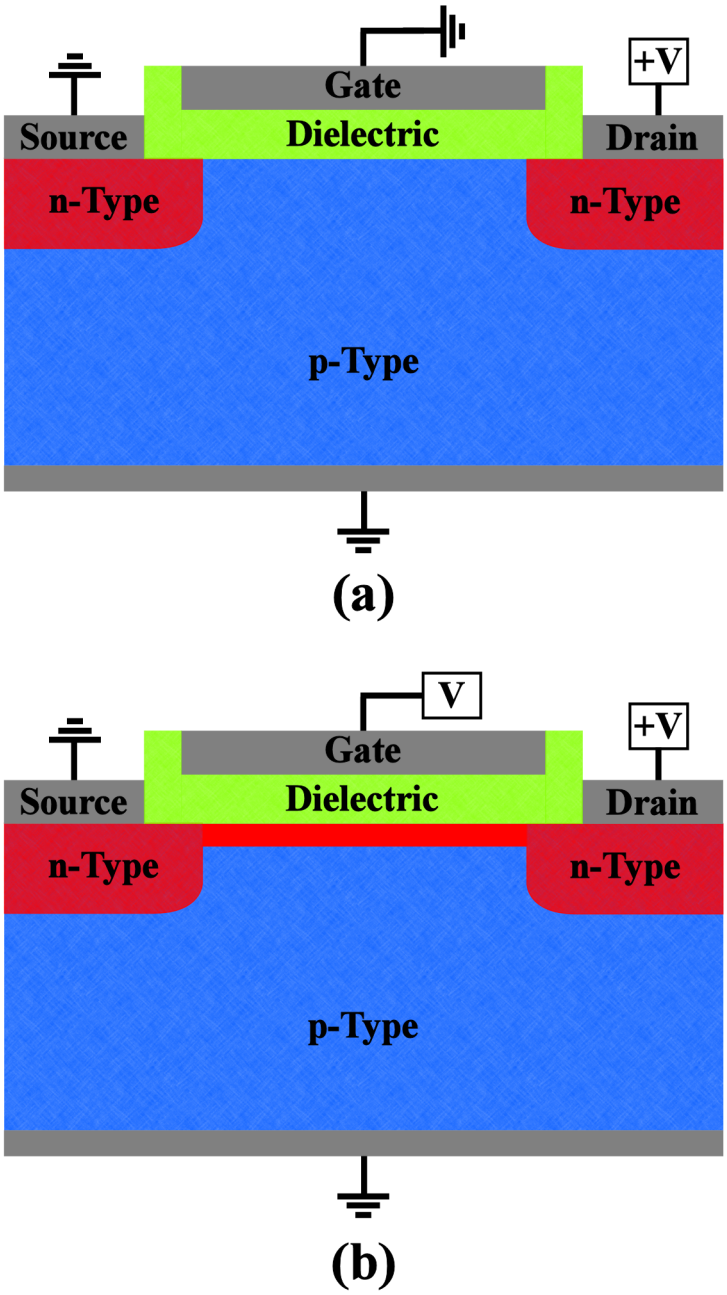

Figure 1.4: Schematic showing a very basic MOSFET device. (a) Shows the MOSFET with no voltage applied to the gate electrode. This prevents any current from flowing from the source to the drain. (b) Shows the MOSFET with a positive voltage applied to the gate electrode. This puts the p-type semiconducting material into inversion near the gate dialectic creating a channel through which current can flow from the source to the drain.

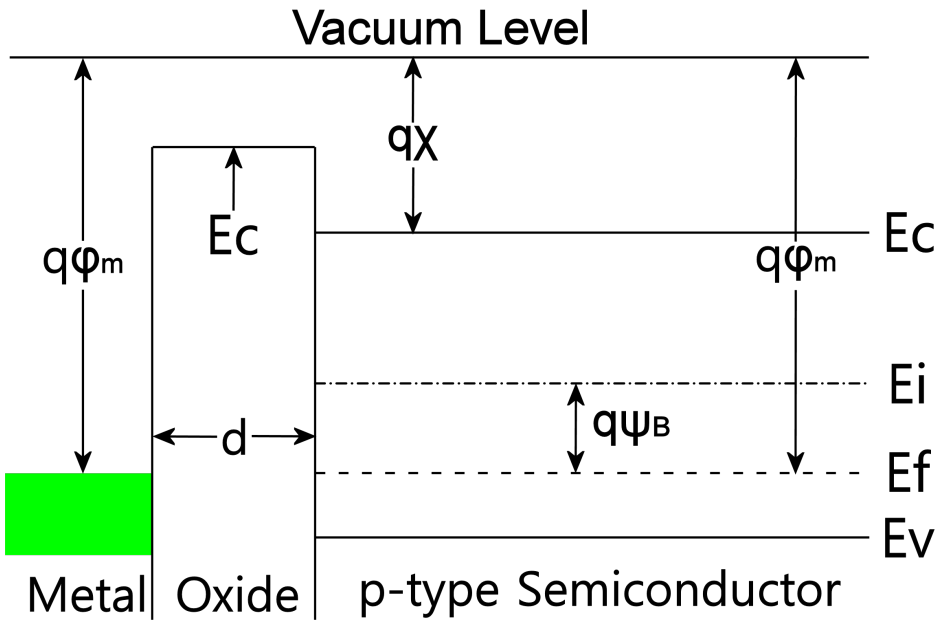

Figure 1.5: Energy diagram of the MOS structure of the MOSFET discussed in Figure 1.4.

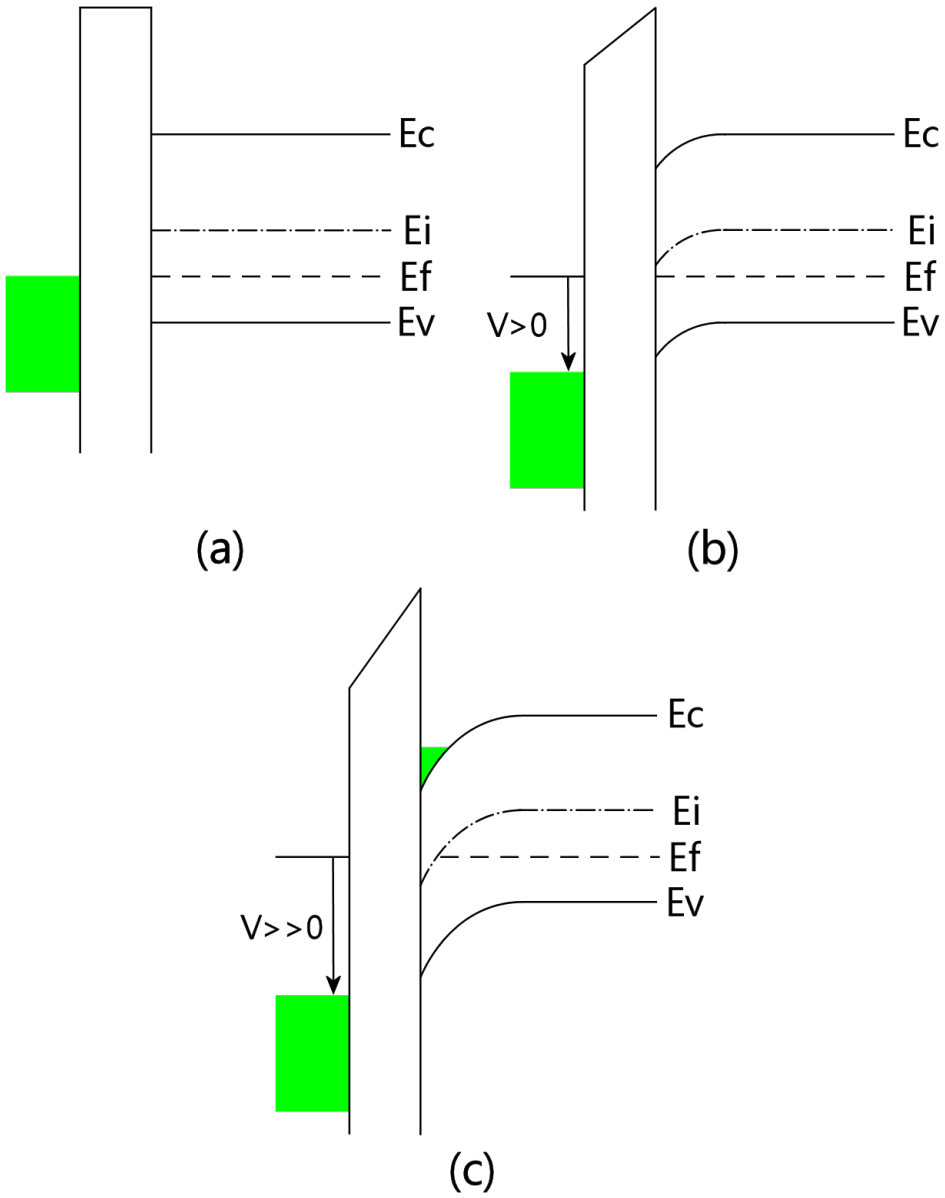

Figure 1.6: Simplified energy diagram of the MOS portion of the MOSFET shown in Figure 1.4. (a) shows the MOS structure at flat band, with no voltage applied to the gate electrode. (b) small positive voltage applied to the gate electrode creating a depletion region in the p-type semiconductor. (c) large positive voltage applied to the gate electrode creating an inversion layer in the p-type semiconductor at the semiconductor dielectric interface. The inversion has allowed electrons into the conduction band of the p-type semiconductor and corresponds to the condition in figure 1.4b in which current is allowed to flow from the source of the MOSFET to the drain.

semiconductor MOS portion of the MOSFET structure, which corresponds with the MOSFET shown in Figure 1.4a (no voltage applied to the gate). In Figure 1.6b shows the MOS structure with a small positive voltage applied. The small positive voltage creates a depletion layer in the semiconductor near the gate dielectric. This creates a region in the semiconductor in which the majority carriers are pushed away from the gate dielectric, however electrons are still not able to flow from the source to the drain. Figure 1.6c shows the p-type semiconducting region when a larger positive voltage has been applied creating a carrier inversion directly under the gate dielectric. This inversion layer in the channel region allows current to flow from the source to the drain, turning the MOSFET on. For further information on MOSFETs and the physics of semiconductor devices see reference number [14].

Under ideal conditions and with perfect materials the MOSFET will work as described above with the device switching from the on state to the off state with no ambiguity as to whether current should or should not be flowing through the MOSFET channel. However several problems arise due to the inevitable imperfections in the MOSFET gate dielectric. The main causes of undesirable functioning due to defects in the gate dielectric are mobile ionic charge, fixed oxide charge, interface trapped charge and oxide trapped charge.[14] The mobile ionic charges are typically due to alkali ions in the gate dielectric that become mobile under high fields or temperatures greater than approximately 100 ^{o}C. The motion of the mobile charge through the gate dielectric can cause shifts in the I-V characteristics of the device.[14] The fixed oxide charge is caused by SiO_2 defects typically located within a few nanometers of the Si-SiO_2 interface and with an areal density of 10^{10} cm^{-2} for carefully prepared SiO_2 gate dielectrics. Under normal operating conditions these defects remain fixed and cannot be charge and discharged. It has been suggested that these fixed charges are due to incomplete oxidation of the Si, which leaves ionic Si near the Si-SiO_2 interface.[14] The interface trapped charges are due to incomplete Si-Si or Si-O bonds at the Si-SiO_2 interface, and typically have energies within the silicon band gap. In modern devices the interface trapped charge is mostly passivated

through thermal growth techniques and hydrogen annealing. This produces defect densities as low as 10^{10} cm^{-2}.[14] Oxide trap states are the last main source of poor device operation due to gate dielectric imperfections and can cause a pathway by which charge carriers can hop through the dielectric film, raise or lower the device threshold voltage and reduce carrier mobility in the channel.[14, 15, 16] These defects are the type of imperfection that can readily be addressed by single electron tunneling force microscopy.

1.6 Electron and Hole Traps in Dielectric Materials

The defects that hinder the operation of electronic devices are typically those with energies that lie within the band gap of the dielectric material. The trapping of electrons or holes by these defects locally charges the oxide and causes unreliable operation of the MOSFET, as was mentioned in the last section. Although there are far too many defects, both measured and predicted theoretically, to mention in this introduction there is one important defect of note that should be briefly mentioned since it will be of particular interest in a later chapter. This defect is known as the E' center, which is an oxygen vacancy on a typical four coordinated Si atom. There is some minor debate as to the make-up of the E' center[17, 18] but it is generally thought to consist of one singly occupied silicon dangling bond and one silicon dangling bond that has trapped a hole making the defect positively charged.[19, 20] The silicon with the trapped hole puckers so that it withdraws behind the plane of the other three oxygen atoms it is bonded to. This oxygen vacancy defect can also exist as neutral with both Si dangling bonds occupied and as the V_O^{2+} in which both Si atoms have absorbed a hole.[18, 19, 20, 21] For an extensive discussion of the E' center as well as numerous other defects found in SiO_2, Si_3N_4 and HfO_2 see references [17, 18, 21, 22, 23, 24].

The characterization of trap states in dielectric materials has been undertaken for decades using numerous techniques, which include I-V,[25, 26, 27] charge pumping,[28] capacitance measurements[29] and optical absorption.[30, 31, 32, 33] Unfortunately

these standard techniques do not allow for characterization of trap states with atomic scale spatial resolution, or the characterization of single trap states in dielectric materials. STM has been used to characterize trap states in thin film dielectrics with atomic scale spatial resolution.[34, 35, 36, 37] However, as was stated earlier the need for a constant current of at least 1 pA requires that the dielectric material be either very thin or have a large enough number of defect states. SETFS is thus well suited to provide new information about trap states in dielectric materials that has not been available due to the limitations of more traditional techniques.

1.7 References

[1] G. Binnig, H. Rohrer, C. Gerber and E. Weibel, Phys. Rev. Lett. 49, 57 (1982)

[2] H. P. Lang, R. Wiesendanger, V. Thommen-Geiser and H.-J. Guntherodt, Phys Rev B 45, 4 (1992)

[3] H. Watanabea, T. Baba and M. Ichikawa, J. Appl. Phys. 87, 11 (2000)

[4] M. J. Romero and J. van de Lagemaat, Phys. Rev. B 80, 115432 (2009)

[5] U. Dürig, Appl. Phys. Lett., 75, 3 (1999)

[6] D. Sarid, Scanning Force Microscopy with Applications to Electric, Magnetic, and Atomic Forces (Oxford University Press, New York, 1994)

[7] F. J. Giessibl, Phys. Rev. B 56, 24 (1997)

[8] L. J. Klein and C. C. Willaims, J. Appl. Phys. 95, 2547 (2004)

[9] E. Bussman, Single Electron Tunneling Force Microscopy, Thesis, University of Utah (2006)

[10] N. Zheng, C. C. Williams, E. G. Mishchenko and E. Bussmann, J. of Appl. Phys. 101, 093702 (2007)

[11] L. J. Klein, C. C. Williams and J. Kim, Appl. Phys. Lett. 77, 22 (2000)

[12] E. Bussmann, Dong Jun Kim and C. C. Williams, Appl. Phys. Lett., 85, 13 (2004)

[13] E. Bussmann and C. C. Williams, Appl. Phys. Lett., 88, 263108 (2006)

[14] S. M. Sze, Semiconductor Devices, Physics and Technology, 2nd edition, John Wiley & Sons, Inc 2002

[15] G. D. Wilk, R. M. Wallace and J. M. Anthony J. Appl. Phys. 89, 5243 (2001)

[16] Z. Xu, M. Houssa, S. De Gent and M. Heyns Appl. Phys. Lett. 80, 1975 (2002)

[17] E. P. O'Reilly and J. Robertson Phys. Rev. B 27, 6 (1983)

[18] C. J. Nicklaw, Z.-Y. Lu, D. M. Fleetwood, R. D. Schrimpf and S. T. Pantelides, IEEE Transactions on Nuclear Science 49, 6 (2002)

[19] H. S. Witham and P. M. Lenahan, Appl. Phys. Lett. 51, 13 (1987)

[20] J. F. Conley Jr., P. M. Lenahan, H. L. Evans, R. K. Lowry and T J. Morthorst, J. Appl. Phys. 76, 5 (1994)

[21] J. Robertson, J. Appl. Phys. 54, 8 (1983)

[22] J Robertson and M. Powell, Appl. Phys. Lett. 44, 4 (1984)

[23] K. Xiong, J. Robertson, M. C. Gibson and S. J. Clark, Appl. Phys. Lett. 87, 183505 (2005)

[24] J. Roberston, Rep. Prog. Phys. 69, 327-396 (2006)

[25] G. Bersuker, J. H. Sim, C. S. Park, C. D. Young, S. V. Nadkarni, R. Choi, and B. H. Lee, IEEE Transactions on Device and Materials Reliability 7, 1 (2007)

[26] C. D. Young, Y. Zhao, D. Heh, R. Choi, B. H. Lee, and G. Bersuker, , IEEE Transactions on Electron Devices 56, 6 (2009)

[27] G. Ribes, S. Bruyère, D. Roy, C. Parthasarthy, M. Müller, M. Denais, V. Huard, T. Skotnicki, and G. Ghibaudo, IEEE Transactions on Device and Materials Reliability 6, 2 (2006)

[28] A. Kerber and E. A. Cartier, IEEE Transactions on Device and Materials Reliability 9, 2 (2009)

[29] M. Placidi, A. Constant, A. Fontserè, E. Pausas, I. Cortes, Y. Cordier, N. Mestres, R. Pérez, M. Zabala, J. Millán, P. Godignon, and A. Pérez-Tomás, Journal of The Electrochemical Society, 157 (11) H1008-H1013 (2010)

[30] E. E. Hoppe and C. R. Aita, APL, 92, 141912 (2008)

[31] J. W. Park, D. K. Lee, D. Lim, H. Lee, and S. H. Choi, JAP, 104, 033521 (2008)

[32] J. Price, P. S. Lysaght, S. C. Song, H. J. Li and A. C. Diebold , APL, 91, 061925 (2007)

[33] N. V. Nguyen, A. V. Davydov, D. Chandler-Horowitz and M. M. Frank , APL, 87, 192903 (2005)

[34] Q. Cai, Y. F. Hu, S. T. Hu, and X. Wang, J. Vac. Sci. Technol B 18(5), Pg. 2384 Sep/Oct 2000

[35] H. Watanabe, Toshio Baba and M. Ichikawa , JAP, 87, 1 (2000)

[36] N. Miyata and M. Ichikawa, Phys. Rev. B, 70, 073306 (2004)

[37] H. F. Cheng, Y. C. Lee, S. J. Lin, Y. P. Chou, T. T. Chen and I. N. Lin, JAP, 97, 044312 (2005)

CHAPTER 2

LOCALIZED DEFECT STATES IN SILICON DIOXIDE AND SILICON NITRIDE FILMS

2.1 Local Apparent Density of Trap States in SiO_2 and Si_3N_4 Films Studied by Single Electron Tunneling Force Spectroscopy

This chapter contains a paper that was published in Journal of Applied Physics (jap.aip.org) Vol. 110, Num. 114102 (2011) entitled *Local density of trap states in SiO_2 and Si_3N_4 films studied by single electron tunneling force spectroscopy* by Dustin Winslow and Clayton Williams.[1] The paper discusses a novel spectroscopy technique developed in the Williams lab, which was used to characterize electron and hole trap states in SiO_2 and Si_3N_4. The paper has been reformatted to match the format of this dissertation.

The local apparent density of trap states measured by the Single Electron Tunneling Force Spectroscopy (SETFS) technique are compared to the theoretically predicted trap state energies found in the literature. Additionally the spectra measured by SETFS is compared to the density of trap states measured by traditional measurement techniques and reported in the literature. The SETFS spectra is shown to be in good agreement with the experimental and theoretical literature and additionally identifies several states that have not been reported in the experimental literature.

It should be noted that the paper contained in this chapter was published after the paper discussed in the next chapter. This reordering was done to preserve the

---

[1]Reprinted with permission from Journal of Applied Physics 110, 114102. Copyright 2011, American Institute of Physics.

flow of the chapters in the dissertation.

2.1.1 Abstract

Standard methods used to characterize defect states in dielectric films generally provide spatially averaged defect information. The development of single electron tunneling force spectroscopy provides for the measurement of local apparent density of trap states with atomic scale spatial resolution. In this article, local apparent density of trap states measurements recently obtained on both silicon dioxide and silicon nitride are presented. Local apparent density of states data observed by this method varies from one location to another. The local spectra are compared with previous measurements and theoretical predictions found in the literature.

2.1.2 Introduction

Silicon dioxide (SiO_2) and silicon nitride (Si_3N_4) have been used as dielectric films in electronic devices for decades and have been studied extensively during this time.[1] Many standard techniques have been applied to characterize the trap states in the band gap of these dielectric films, including I-V,[2, 3, 4], charge pumping,[5] capacitance measurements[6] and optical absorption.[7, 8, 9, 10] However, these techniques do not typically provide information about the atomic scale spatial distribution of the trap states. Additionally, many do not probe trap states that lie near the conduction or valence bands or states very near the surface of the dielectric.

Nanometer scale measurements have been made on dielectric films using a scanning tunneling microscope (STM).[11, 12, 13, 14] However STM requires very thin films or a high enough density of defect states to allow for a measurable current between the tip and substrate. These requirements limit the ability of an STM to measure defect states in thicker dielectric films, or to characterize single, electrically isolated defect states.

Single electron tunneling force spectroscopy (SETFS)[15, 16, 17] was developed to characterize electrically isolated trap states with atomic scale spatial resolution. SETFS allows the energy of single defect states within the band-gap to be probed

on nonconductive films with subnanometer spatial resolution by varying the applied voltage between the tip and sample substrate. As the voltage applied between the metalized AFM probe tip and the sample is varied, electrons are able to elastically tunnel into (and out of) electronic trap states[16, 17, 18] (see Figure 2.1). Any charge which has tunneled to (or from) the surface modifies the surface potential of the sample and creates an additional force gradient on the tip, shifting the resonant frequency of the AFM cantilever, and enabling detection of the tunneling events.

Another AFM based method has also demonstrated single electron tunneling to prepared quantum dots and trap states in thick dielectric films.[19, 20] However, this method relies on tunneling from the sample substrate, and therefore does not provide atomic scale spatial resolution.

2.1.3 Method

The SiO_2 sample used in this study is a 10 nm thick film, grown on a p-type Si substrate. The Si_3N_4 sample used is a 20 nm thick film grown on a n-type Si substrate. The SETFS measurements are performed in vacuum (~10^{-9} Torr). Each sample is prepared by ultrasonic cleaning in acetone and isopropyl alcohol, after which the sample is rinsed with de-ionized water and blown dry with nitrogen. Once in the UHV chamber, the sample is heated to 350 °C for 45 minutes to drive off any organic material on the sample surface. After the sample is cooled to room temperature in vacuum, the tip is moved to a height of 5.4 nm above the sample surface and an AC square wave (3 V_{peak} at ~ 300 Hz) is applied to measure the surface potential of the sample.[17, 21] A DC offset voltage applied to the sample is adjusted until the flatband condition is reached (average tip potential equal to sample surface potential). Once the flatband condition is achieved, the AC square wave is turned off and the system is ready to start the spectroscopic measurements.

Under ideal conditions (uncharged, atomically clean surface) the voltage required to reach flatband is only dependent on the work function (Φ) of the metal of the tip and the electron affinity of the dielectric material (χ). The tip used during the measurements has a platinum coating with work function $\Phi_{Pt} = 5.65$ eV.[22]

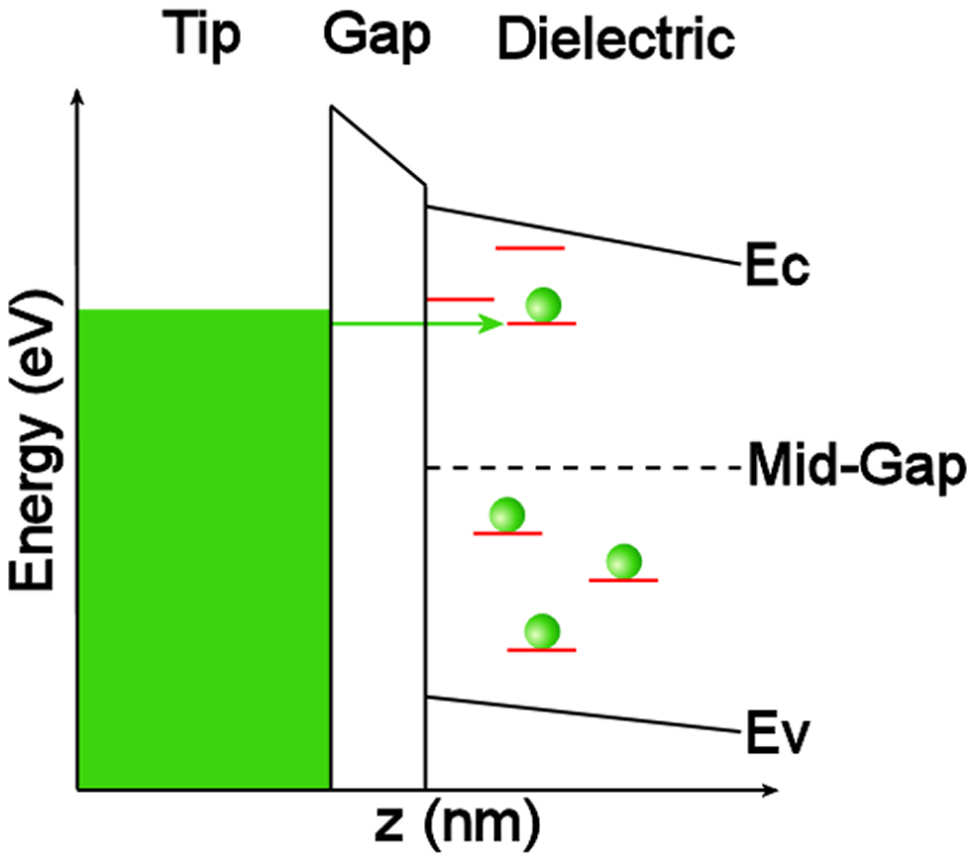

Figure 2.1: Illustration showing states in the band gap of the dielectric that satisfy the conditions for tunneling. Lines indicate trap states. Circles indicate filled states. As the voltage applied to the sample is varied, the electrons elastically tunnel between the states in the metal tip and the defect states in the dielectric film.

The electron affinity for SiO_2 is $\chi_{SiO2} = 0.8$ eV.[23] This puts the Fermi level of the platinum tip 0.35 eV below the middle of the band gap of SiO_2. The electron affinity for Si_3N_4 is $\chi_{Si3N4} = 2.1$ eV,[24] which places the Fermi level of the tip 0.9 eV below the Si_3N_4 mid-gap. However since the samples used in this experiment were not prepared to be atomically clean ($\sim 10^{-9}$ Torr), it has been assumed that, at the measured flatband voltage, the Fermi level of the tip is approximately at the middle of the band gap for both dielectric films.

A graphical representation of the SETFS methodology can be seen in Figure 2.2, which shows the case for electron injection, from tip to sample. However, the same principles apply to the electron extraction case (negative applied voltages). All voltages are applied to the sample with respect to the voltage required to reach flatband. The spectroscopy measurements are started immediately after the aforementioned flatband adjustment (5.4 nm tip/sample gap). To perform the spectroscopic measurements, the tip is placed at the measurement location and the AC square wave is applied to measure the local surface potential, and is then turned off. A DC tunneling voltage (V_{App}) is applied to the sample, and the tip/sample gap is reduced to 0.8 nm (tunneling range). If an empty trap state exists in the dielectric film, at or below the Fermi-level of the probe, an electron will elastically tunnel from the tip to the sample. After a 30 ms tunneling attempt time, the tip is retracted (5.4 nm, out of tunneling range) and the DC voltage is turned off. The AC square wave is again applied between the tip and sample to measure the surface potential. The difference in surface potential before and after the tunneling attempt is directly proportional to the number of electrons that tunneled during the tunneling attempt. This cycle is then repeated, with incrementally larger applied tunneling voltages. The differential surface potential before and after each tunneling attempt, plotted against the tip-surface gap voltage, provides the relative apparent density of trap states in the band gap.

To establish a proper energy scale for these measurements the applied voltage must be scaled to the voltage dropped across the tip-sample gap. To accomplish

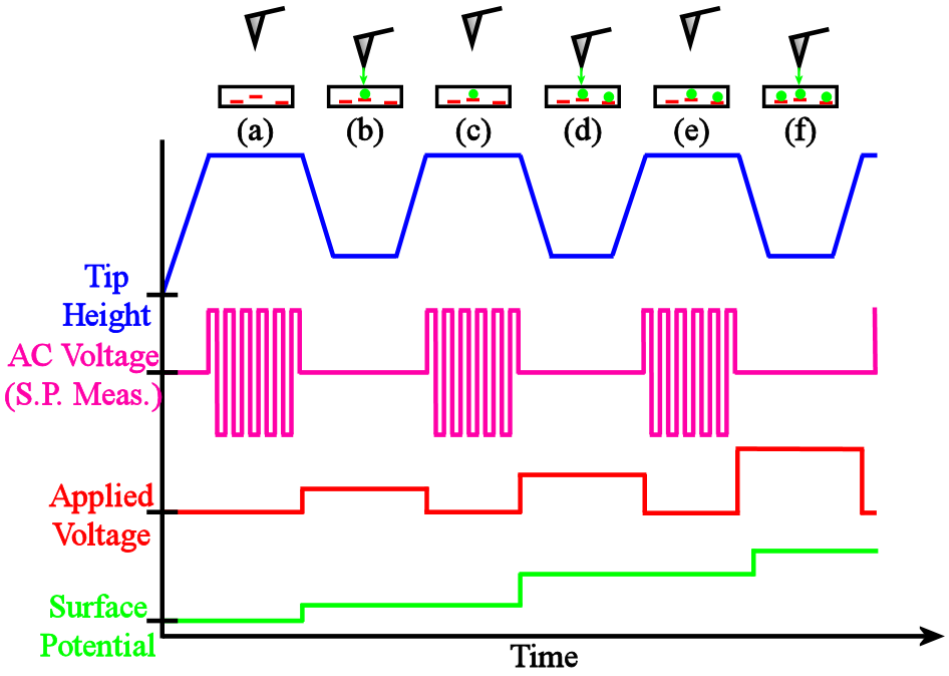

Figure 2.2: Diagram showing the applied voltages as a function of time. The energy spectrum of band gap states are probed by (a) first increasing the sample/tip gap to 5.4 nm and turning on an AC square wave to measure the surface potential. (b) The AC square wave is turned off and a DC voltage is applied to the tip to induce tunneling. The tip is brought into tunneling range of the sample and is stopped at a minimum tunneling gap (0.8nm). The tip sits at the minimum gap for a dwell time of 30 ms after which the tip is again moved out to 5.4 nm and the DC voltage is turned off. (c) The surface potential is again measured and the cycle is repeated with increasing applied voltages (d-f).

this, a parallel plate capacitor model[17] is applied. In this one-dimensional model, the voltage dropped between the tip and trap states at the surface is given by

$$V_{gap} = \frac{z}{z + \frac{t}{k}} V_{APP} \tag{2.1}$$

where z is the minimum tunneling gap, t is the dielectric thickness (10 nm and 20 nm for SiO_2 and Si_3N_4, respectively), k is the dielectric constant (3.9 and 7 for SiO_2 and Si_3N_4, respectively)[1] and V_{App} is the voltage applied to the sample with respect to the flatband voltage. This one dimensional model has been shown to be adequate for these measurements.[18]

During this study, the trap states in the band gap are probed by first applying a tunneling voltage of 0 V to the sample, with respect to flatband. The applied tunneling voltage is then incrementally increased (decreased) in 2 V steps until, for the case of the SiO_2, + 20 V (-20 V) is reached, and in the case of the Si_3N_4, +14 V (-14 V) is reached. Using the scaling model with the conditions described above, these voltages produce a tip-surface gap voltage of +4.76 V (-4.76 V) for SiO_2 and +3.06 V (-3.06 V) for Si_3N_4, which places the tip Fermi-level just above (below) the conduction (valence) mobility edges. This scaling indicates that the apparent density of states is sampled with an energy step size (gap voltage step size) of 0.48 eV in the SiO_2 measurements and and 0.44 eV for the case of Si_3N_4.

2.1.4 Results and Discussion

SETFS measurements were taken at many locations on both the SiO_2 and Si_3N_4 samples. The relative apparent density of states is found by differentially subtracting the surface potential values before and after each tunneling attempt. In Figure 2.3, six local apparent density of trap state curves can be seen for SiO_2. Note that the error at each point in the individual spectrum is smaller than the data points shown.

Above mid-gap several peaks are easily identified. The green curve (square) shows a peak at 4.1 eV, which corresponds nicely with a defect state predicted by O' Reilly *et al.*[25] This predicted state has also been identified by optical absorption.[26] Slightly lower in energy two peaks can be seen in both the black curve (circle) and red curve

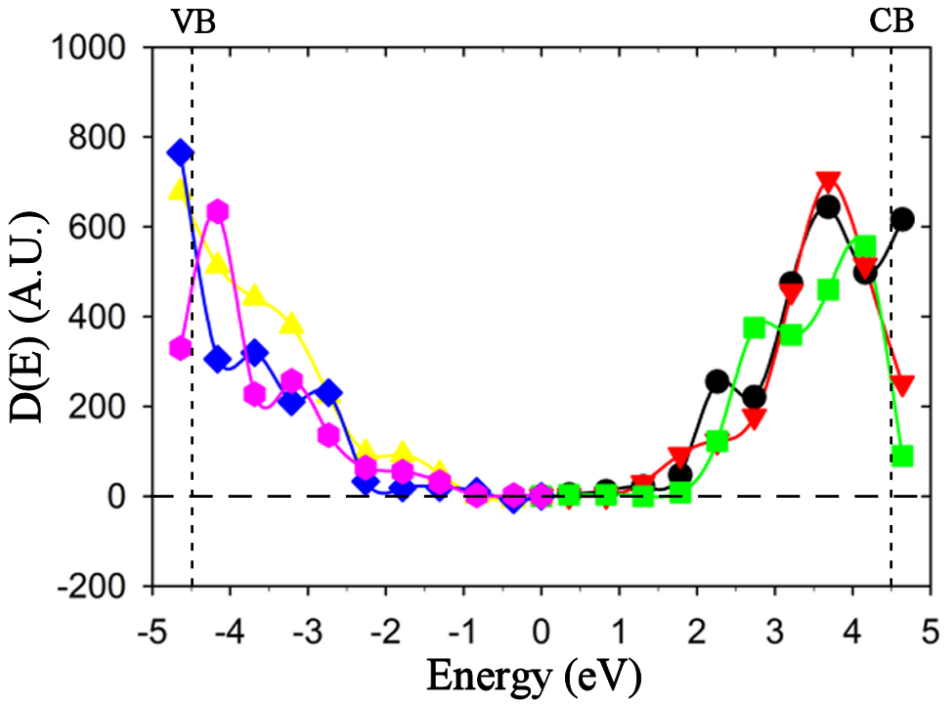

Figure 2.3: Six representative plots (three above and three below mid-gap) of the local apparent density of trap states in the SiO_2 band gap.

(down triangle), at approximately 3.7 eV. There is no experimental evidence in the literature that points to the existence of this state. We believe, however, that this 3.7 eV peak may be the same state we identified at 4.1 eV, but physically deeper in the oxide. This can be justified by using the analysis described in the paper by Johnson.[27] The energy scale used in these measurement is calculated using the voltage dropped between the tip and the trap state. Since the depth of the states is unknown, an assumption is made that the trap states are at the sample surface, which does not take into account the additional voltage dropped in the oxide (between the sample surface and the deeper states). This causes a deeper state to "appear" at a scaled energy which is closer to the middle of the gap than its actual energy.[27] If the 4.1 eV state is approximately 0.5 nm below the sample surface, it will appear at an energy of 3.7 eV during the spectroscopy measurements.

Two more peaks, one at 2.8 eV in the green curve (square) and one at 2.4 eV in the black curve (circle), do not correspond with any experimental data in the literature, however they do line up with defects predicted theoretically to be between 1 eV and 2 eV below the SiO_2 conduction band.[25] It is also possible that these peaks are due to the 4.1 eV state but at an oxide depth approximately 2.5 nm below the sample surface. The red curve (down triangle) also has a shoulder that spans from 1.5 eV to about 2.5 eV. This shoulder lines up nicely with the state found by photon stimulated tunneling I-V curves.[28] It should be noted that additional states predicted to be just above the middle of the band gap[25, 29] are not observed in these SETFS measurements. These states are predicted to exist near the Si-SiO_2 interface. Due to the 10 nm thickness of the SiO_2 film, these states are out of tunneling range.

Below mid-gap in both the blue (diamond) and pink (hexagon) traces there is a small shoulder from approximately -1.5 eV to -2.2 eV. This shoulder may be associated with a state 2.1 eV from the valence band that was predicted by O' Reilly and Robertson.[25] The blue curve (diamond) has additional peaks at both -2.8 eV and -3.6 eV with a peak separation of about 0.8 eV. The pink curve (hexagon) has a peak at both -3.2 eV and -4.2 eV with a separation of ˜1.0 eV. These peaks are

likely due to states that can take a range of energies depending on bond length, which were previously predicted by Nicklaw *et al.*[29] The yellow curve (up triangle) corroborates the idea that the states near the valence band cover a range of energies as no single identifiable peaks can be seen. The existence of several closely spaced defect states near the valence band has also been predicted by O' Reilly *et al.*[25] Several luminescence bands have been correlated to these predictions.[30, 31]

Figure 2.4 shows the SiO_2 apparent density of states averaged over measurements taken at 60 locations on the sample. The error bars indicate the standard deviation for each data point. The larger apparent noise in the average spectra as compared to the individual spectrum is because of the variation between each individual measurement area. Additionally not all spectrum were taken with the same AFM tip. The difference in tip sample interaction, due to the various tips, also contributes to the greater error in the averaged spectrum. Above mid-gap, individual peaks have become indiscernible and only a single broad peak is apparent. This inhomogeneous broadening is due to spatial averaging over local variations in the film and over depth shifted state energies. The peak, however, corresponds nicely with the state predicted by theory[25], at 4.1 eV, and identified by optical absorption.[26]

Below mid-gap, any evidence of the individual peaks is washed out as well. The average fits nicely with previous theory, which predicts many, closely spaced (in energy) states a few eV below mid-gap.[25, 29]

Figure 2.5 shows six apparent density of trap states curves for Si_3N_4. Again the error at each point in the individual spectrum is smaller than the data points shown. All measured apparent density of states curves taken above mid-gap show a peak at approximately 2.3 eV. The fact that this peak is always found at 2.3 eV implies that it is likely due to a true surface state, and does not occur deeper in the oxide. As was discussed earlier, when a state exists at a greater depth, its apparent energy is shifted toward the middle of the gap. The 2.3 eV state observed in the data below is likely the one predicted by Pacchioni *et al.*, which was found using Density Functional Theory (DFT) to be 4.9 eV above the Si_3N_4 valence band.[32] This would put the

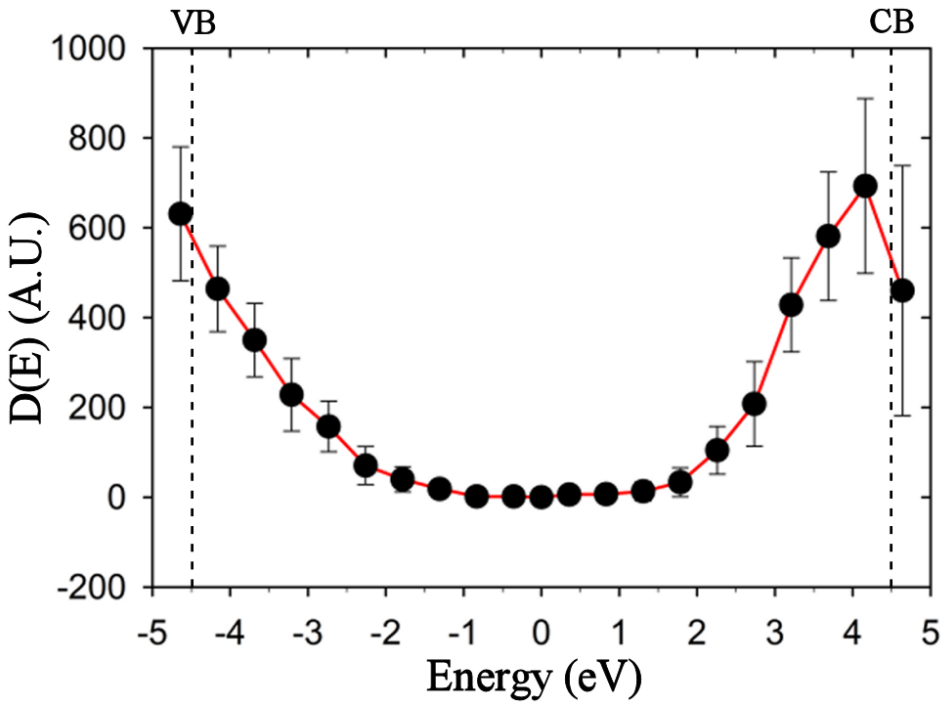

Figure 2.4: Spatially averaged apparent density of states for SiO_2. The spectrum is the average of 60 local measurements obtained at different locations on the sample surface. The error bars indicate the standard deviation from the mean for each data point.

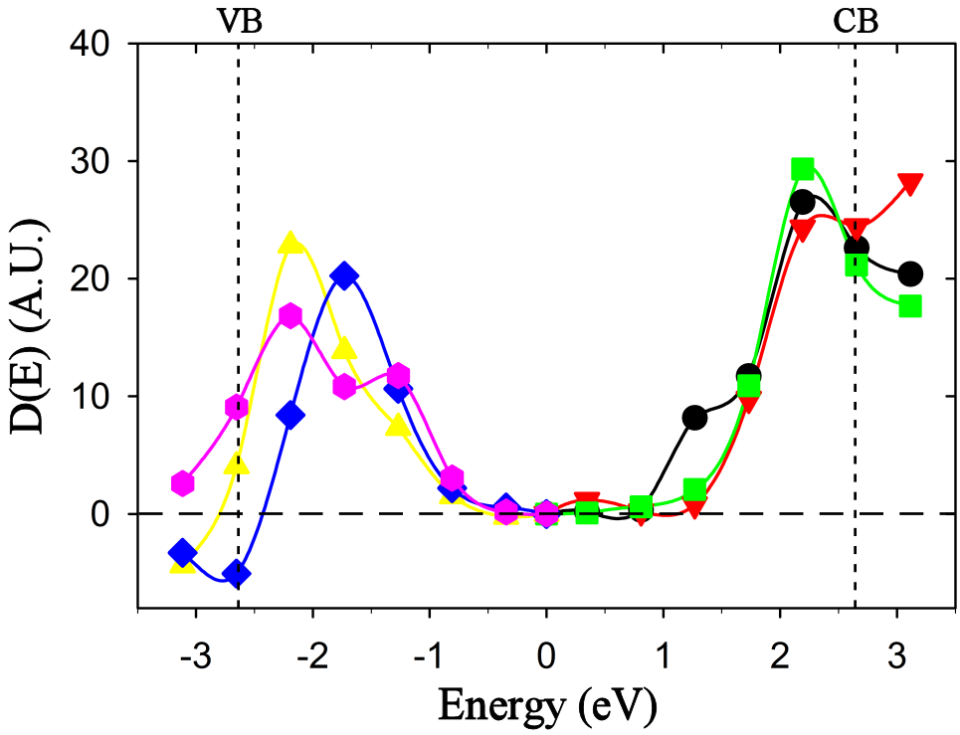

Figure 2.5: Six representative plots (three above and three below mid-gap) of the relative apparent density of trap states in the Si_3N_4 band gap.

state 2.25 eV above the middle of the band gap, matching well to the obvious peak at 2.3 eV in Figure 2.5. This state is a dangling bond surface state similar to the one found at the surface of SiO_2.[32] This may explain why the individual measured apparent density of states curves have a sharp peak at approximately 2.3 eV.

About one half of the spectra obtained at different locations show a shoulder from about 1.2 eV to 1.5 eV (Figure 2.5). This shoulder may be the state predicted by Robertson[33] at 4.2 eV above the valence band, which would be 1.6 eV above the middle of the gap. This would place the state within the 0.44 eV sampling resolution of our data. Another very small peak can be seen in one of the spectra (downward triangle) at about 0.5 eV above mid-gap. This peak appeared in about one third of the spectra and may be a state predicted by theory[33] and measured experimentally[34] to be at 0.5 eV above the middle of the band gap.

Below mid-gap there are three readily identifiable peaks. The pink curve (hexagon) shows two peaks, one at -1.3 eV below mid-gap and the other at -2.2 eV below mid-gap. The yellow curve (up triangle) has evidence of the -1.3 eV peak (as a very small shoulder) and an obvious peak at -2.2 eV. The blue curve (diamond) shows a peak at -1.6 eV. The peak at -2.2 eV shows up in about one third of the spectra and lines up very nicely with a state that has been predicted by theory.[33] The existence of this type of defect, a singly occupied nitrogen vacancy, has been confirmed by EPR.[35] The -1.6 eV peak appears four times in the 30 spectra taken below mid-gap. Additionally a series of broad peaks (not shown) between -1.5 eV and -2.2 eV appear in approximately one third of the spectra taken. Given the 0.44 eV energy sampling step size, it is likely that the series of broad peaks along with the identifiable peaks at -1.6 eV are likely due to versions of the -2.2 eV state at physically greater depths in the Si_3N_4 film. The -1.3 eV peak occurs either as a single peak or shoulder in one half of the spectra taken, and is evidence of a state -1.3 eV below the Si_3N_4 mid-gap. In each instance of this peak there is no evidence of depth broadening, which implies that the state is likely a true surface state. Additionally the -1.3 eV peak cannot be due to a physically deeper version of the nitrogen vacancy state that was detected

at -2.2 eV, because the depth required to produce this energy shift would put the state out of tunneling range. Evidence of a state at -1.3 eV, either theoretical or experimental, was not found in the literature.

Figure 2.6 shows the spatially averaged Si_3N_4 apparent density of states obtained at 60 locations on the sample. The error bars indicate the standard deviation for each data point. As with the averaged SiO_2 spectra shown in Figure 2.4, the averaged Si_3N_4 spectrum shown in Figure 2.6 is quite broad and does not show the individual peaks observed in Figure 2.5. Only a single broad peak centered at about 2.3 eV above mid-gap is seen, which is at the energy of the state earlier posited to be a true surface state. There is a clear peak centered around -1.9 eV below mid-gap. This peak could be associated with states at -2.2 eV,[33] but broadened by a range of physical depths in the film.

2.1.5 Conclusion

Apparent density of states measurements have been acquired with atomic scale spatial resolution using single electron tunneling force spectroscopy, on both silicon dioxide and silicon nitride films. A spatial variation in the apparent density of trap states in both films is apparent from the data. Many states in both films have been linked to corresponding states observed by other experimental methods or predicted by theoretical calculations. A variation in state depth has been posited to explain the tendency of some peaks to appear at an energy closer to mid-gap than is discussed in the literature. Additionally a state at -1.3 eV below the middle of the gap in Si_3N_4 has been found by single electron tunneling force spectroscopy, which is not found in the literature either experimentally or theoretically, and cannot be explained by depth broadening. It is proposed that this state may be a true surface state.

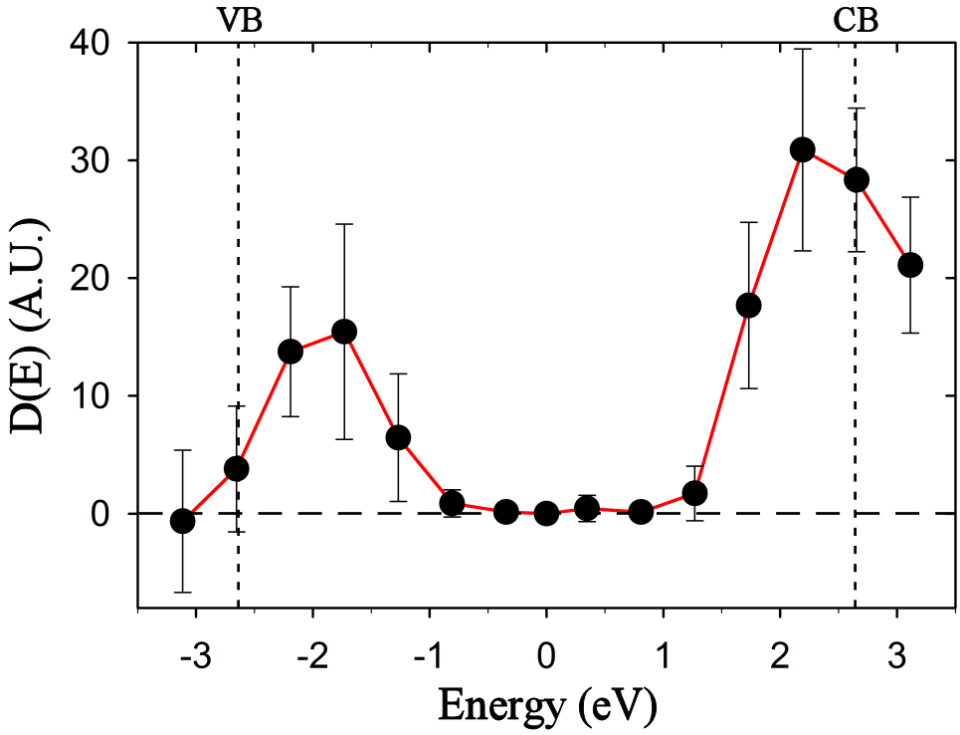

Figure 2.6: Average apparent density of states for Si_3N_4. The spectrum is averaged from 60 individual spectra locations on the sample surface. The error bars indicate the standard deviation from the mean for each averaged data point.

2.2 References

[1] J. Robertson, Rep. Prog. Phys. 69, 327 (2006)

[2] G. Bersuker, J. H. Sim, C. S. Park, C. D. Young, S. V. Nadkarni, R. Choi, and B. H. Lee, IEEE Transactions on Device and Materials Reliability 7, 1, Pg. 138 (2007)

[3] C. D. Young, Y. Zhao, D. Heh, R. Choi, B. H. Lee, and G. Bersuker, , IEEE Transactions on Electron Devices 56, 6, Pg. 1322 (2009)

[4] G. Ribes, S. Bruyère, D. Roy, C. Parthasarthy, M. Müller, M. Denais, V. Huard, T. Skotnicki, and G. Ghibaudo, IEEE Transactions on Device and Materials Reliability 6, 2, Pg. 132 (2006)

[5] A. Kerber and E. A. Cartier, IEEE Transactions on Device and Materials Reliability 9, 2, Pg. 147 (2009)

[6] M. Placidi, A. Constant, A. Fontserè, E. Pausas, I. Cortes, Y. Cordier, N. Mestres, R. Pérez, M. Zabala, J. Millán, P. Godignon, and A. Pérez-Tomás, Journal of The Electrochemical Society 157, 11, H1008-H1013 (2010)

[7] E. E. Hoppe and C. R. Aita, Appl. Phys. Lett. 92, 141912 (2008)

[8] J. W. Park, D. K. Lee, D. Lim, H. Lee, and S. H. Choi, J. Appl. Phys 104, 033521 (2008)

[9] J. Price, P. S. Lysaght, S. C. Song, H. J. Li and A. C. Diebold , Appl. Phys. Lett. 91, 061925 (2007)

[10] N. V. Nguyen, A. V. Davydov, D. Chandler-Horowitz and M. M. Frank , Appl. Phys. Lett. 87, 192903 (2005)

[11] Q. Cai, Y. F. Hu, S. T. Hu, and X. Wang, J. Vac. Sci. Technol B 18, 5, Pg. 2384 (2000)

[12] H. Watanabe, Toshio Baba and M. Ichikawa , J. Appl. Phys. 87, 1 (2000)

[13] N. Miyata and M. Ichikawa, Phys. Rev. B 70, 073306 (2004)

[14] H. F. Cheng, Y. C. Lee, S. J. Lin, Y. P. Chou, T. T. Chen and I. N. Lin, J. Appl. Phys. 97, 044312 (2005)

[15] E. Bussmann, Dong Jun Kim, and C. C. Williams, Appl. Phys. Lett. 85, 2538 (2004)

[16] E. Bussmann and C. C. Williams, Appl. Phys. Lett. 88, 263108 (2006)

[17] N. Zheng, J. P. Johnson, C. C. Williams and G. Wang, Nanotechnology 21, 295708 (2010)

[18] D. W. Winslow, J. P. Johnson and C. C. Williams, Appl. Phys. Lett. 98, 172903 (2011)

[19] R. Stomp, Y. Miyahara, S. Schaer, Q. Sun, H. Guo, P. Grutter, S. Studenikin, P. Poole, and A. Sachrajda, Phys. Rev. Lett. 94, 056802 (2005)

[20] A. Dana and Y. Yamamoto, Nanotechnology 16, S125–S133 (2005)

[21] E. Bussmann, N. Zheng and C. C. Williams 2006 Nano Lett. 6 2577 (2006)

[22] D.E. Eastman, Phys. Rev. B 2, 1 (1970)

[23] V. V. Zhirnov, G. J. Wojak, W. B. Choi, J. J. Cuomo, and J. J. Hren, J. Vac. Sci. Technol. A 15, 3 (1997)

[24] J. Robertson, J. Vac. Sci. B 18, 3 (2000)

[25] E.P. O' Reilly, and J. Robertson, Phys. Rev. B 27, 6 (1983)

[26] N. Terada, and T. Haga, and N. Miyata, and K. Moriki, and M. Fujisawa, and M. Morita, and T. Ohmi and T. Hattori, Phys. Rev. B 46, 4 (1992)

[27] J.P Johnson, D.W. Winslow C.C. Williams, Appl. Phys. Lett. 98, 052902 (2011)

[28] V. V. Afanas'ev, and J. M. M. De Nijs, and P. Balk and A. Stesmans, J. App. Phys. 78, 12 (1997)

[29] C. J. Nicklaw, Z.-Y. Lu, D. M. Fleetwood, R. D. Schrimpf and S. T. Pantelides, IEEE Transactions on Nuclear Science 49, 6 (2002)

[30] H. Sigel and M. J. Marrone, J. Non-Cryst. Solids 45, 235 (1981)

[31] D. L. Griscom, Proc. Freq. Cont. Symp. 37, 98 (1979)

[32] G. Pacchioni and D. Erbetta, Phys. Rev. B. 60, 18 (1999)

[33] J. Robertson, App. Phys. 54, 8 (1983)

[34] S. Jung, D. Gong, and J. Yi, Sol. Energy Mater. Sol. Cells 95, Pg. 546-550 (2011)

[35] W. L. Warren, J. Kanicki, and E. H. Poindexter, Colloids and Surfaces A: Physicochemical and Engineering Aspects 115, Pg. 311-317 (1996)

CHAPTER 3

LOCALIZED DEFECT STATES IN HAFNIUM OXIDE FILMS

3.1 Nanometer Scale Study of HfO_2 Trap States Using Single Electron Tunneling Force Spectroscopy

This chapter contains a paper that was published in Applied Physics Letters (apl.aip.org) Vol. 98, Num. 172903 (2011) entitled *Nanometer scale study of HfO_2 trap states using single electron tunneling force spectroscopy* by Dustin Winslow, Jon Paul Johnson and Clayton Williams.[1] The paper discusses the first measurements made on a dielectric material using a novel spectroscopy technique developed in the Williams lab. The paper has been reformatted to match the format of this dissertation.

The local apparent density of trap states measured in HfO_2 by the Single Electron Tunneling Force Spectroscopy (SETFS) technique are compared to the theoretically predicted trap state energies found in the literature. Additionally the spectra measured by SETFS is compared to the density of trap states measured by traditional measurement techniques and reported in the literature. The SETFS spectra is shown to be in good agreement with the experimental and theoretical literature and additionally identifies states that have not been reported in the experimental literature.

The paper contained in this chapter was published before the paper discussed in the previous chapter. This reordering was done to preserve the flow of the chapters in the dissertation.

---

[1]Reprinted with permission from Applied Physics Letters 98, 172903. Copyright 2011, American Institute of Physics.

3.1.1 Abstract

Standard methods to characterize trap states in dielectric films typically provide spatially averaged measurements. The development of Single Electron Tunneling Force Spectroscopy has provided for the measurement of the energy of single trap states with atomic scale spatial resolution. In this letter, data taken on HfO_2 films using this method is presented and discussed. Analysis of individual spectra shows that there is spatial variation in the apparent density of trap states in these films. The spectra found by averaging data obtained from forty different locations shows good agreement with data taken via standard methods and with theoretical predictions.

3.1.2 Article

High-K dielectric materials play a critical role in modern electronic devices, having been introduced to continue the scaling of device size.[1] Various techniques have been developed to characterize trap states in dielectric materials, including I-V,[2, 3, 4] charge pumping,[5] capacitance measurements[6] and optical absorption.[7, 8, 9, 10] However the use of these techniques is typically limited to areas much greater than one square micrometer, which cannot provide information about the atomic scale spatial distribution of trap states. Additionally, many of these approaches cannot probe states that lie near the conduction and valence bands.

Nanometer scale measurements can be made on dielectric films using a scanning tunneling microscope (STM).[11, 12, 13, 14] However STM requires very thin films on conducting substrates, or a high enough density of defect states to allow for a measurable current between the tip and substrate. These requirements limit the ability of a STM to measure defect states in thicker dielectric films, and to characterize single, electrically isolated defect states.

Another Atomic Force Microscope (AFM) based method provides for tunneling to single defect states in thick dielectric films.[15, 16] However this method relies on tunneling from the sample substrate to the defect states, and therefore does not allow for atomic scale spatial resolution.

Single Electron Tunneling Force Spectroscopy (SETFS)[17, 18] is based on force

detected single electron tunneling.[19] It was developed to allow for tunneling between electrically isolated trap states and a metalized AFM tip, with nanometer scale resolution. SETFS allows the energy of single defect states within the band gap to be probed on nonconductive films. Figure 3.1 shows that as the voltage between the metalized AFM probe tip and the sample is varied, electrons are able to elastically tunnel into (and out of) trap states. Added charge near or at the surface creates an additional force gradient on the tip, shifting the resonant frequency of the AFM cantilever, and enabling detection of the tunneling events. The change in surface potential is proportional to the number of electrons added to or removed from the surface by tunneling. In this work the SETFS technique is used to probe the apparent density of trap states in a HfO_2 film.

The samples used in this study are 3.2 nm HfO_2 films grown on a 1.5 nm SiO_2 film on a Si substrate. The samples were rapid thermal annealed (RTA) at 1000 °C for five seconds. The SETFS measurements are obtained at room temperature in vacuum (~10^{-9} Torr) using an Omicron Multiprobe S Atomic Force Microscope (AFM) system. Each sample is prepared by ultrasonic wash and rinse in acetone and isopropyl alcohol, after which the sample is rinsed with de-ionized water and blown dry with N_2. Once in the UHV chamber the sample is heated to 350 °C for 45 minutes to drive off any organic material on the sample surface. After the sample is cooled to room temperature, under vacuum, the AFM tip is moved to a height of 5.4 nm above the sample surface and an AC square wave (3 V_{peak} at ~ 300 Hz) is applied to measure the surface potential of the sample using the method described in references [17] and [20]. A DC offset voltage applied to the sample is adjusted until the flatband condition is reached (tip potential equal to surface potential). Once this condition is achieved the AC square wave is turned off and the system is ready to start the spectroscopic measurements.

It should be noted that under ideal conditions (atomically clean surfaces), the flat-band condition is dependent only on the work function of the Pt tip, $\Phi_{Pt} = 5.65$ eV[21], and the electron affinity of the HfO_2, $\chi_{HfO2} = 2.0$ eV[22]. Since the band gap of HfO_2

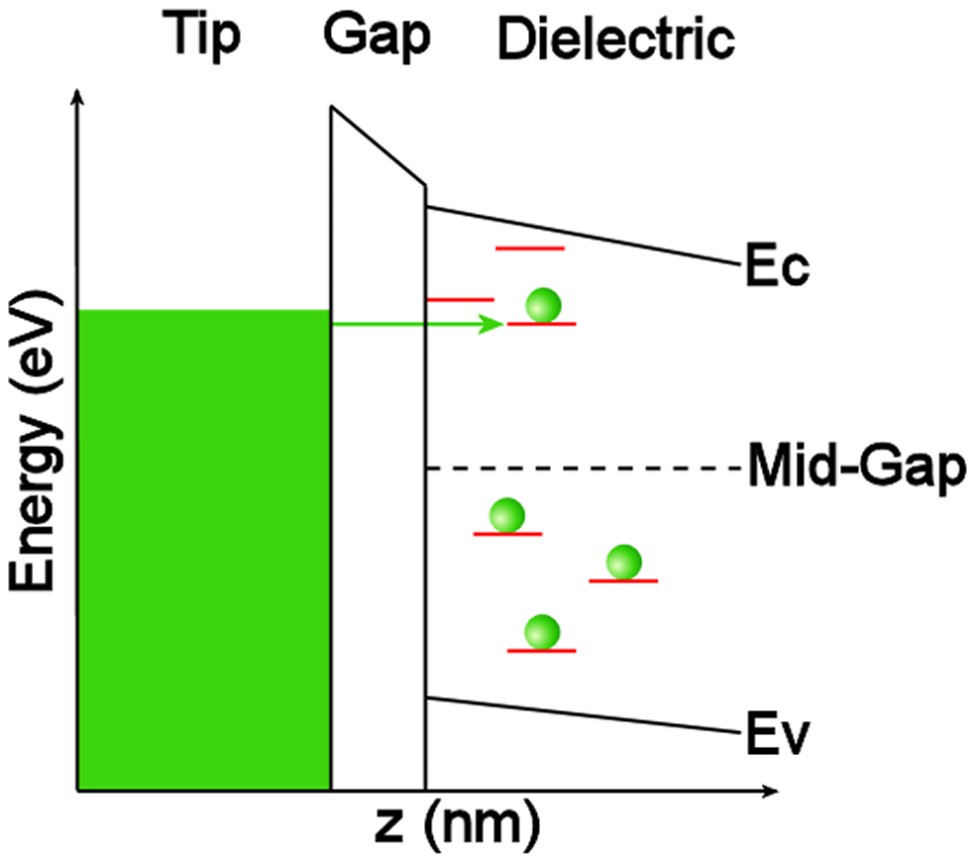

Figure 3.1: States in the band gap that satisfy the conditions for tunneling. Circles indicate filled states. As the voltage applied to the sample is varied, the electrons can elastically tunnel between the metal tip and the trap states in the film.

is ~ 5.8 eV,[1] under these ideal conditions, the Fermi-level of the Pt tip would lie approximately 0.75 eV below the middle of the HfO_2 band gap. Since our tips and samples are not prepared to be atomically clean (chamber pressure 10^{-9} Torr), we have assumed that the Fermi-level of the tip is near the middle of the band gap of the HfO_2 under the flatband condition.

A graphical representation of the methodology can be seen in Figure 3.2, which shows the case of electron injection; however the same principles apply to the extraction case (negative applied voltages). All voltages are applied to the sample with respect to the voltage required to reach flatband. The spectroscopy measurements are started with the tip at a height of 5.4 nm with respect to the sample surface. The AC square wave is applied to measure the surface potential, and is then turned off. A DC tunneling voltage is applied to the sample with respect to the tip, and the tip/sample gap is reduced to 0.8 nm (tunneling range). If an empty trap state exists in the dielectric film, at or below the Fermi-level of the tip, an electron will elastically tunnel from the tip to the sample. After a 30 ms tunneling attempt time, the tip is retracted (5.4 nm, out of tunneling range) and the DC voltage is turned off. The AC square wave is again applied between the tip and sample to measure the surface potential. The difference in surface potential before and after the tunneling attempt is directly proportional to the number of electrons that tunneled during the tunneling attempt. This cycle is then repeated, with incrementally larger applied tunneling voltages. The differential surface potential before and after each tunneling attempt, plotted against the tip-surface gap voltage, provides the relative apparent density of trap states in the band gap. The full band gap is probed by then incrementally increasing (decreasing) the DC tunneling attempt voltage in 1 volt steps until the band edges are reached. To establish a proper energy scale for these measurements the applied voltage must be scaled to the voltage dropped across the tip-sample gap. To accomplish this a parallel plate capacitor model[17] is used. In this one dimensional model, the voltage dropped between the tip and trap states at the surface is given by

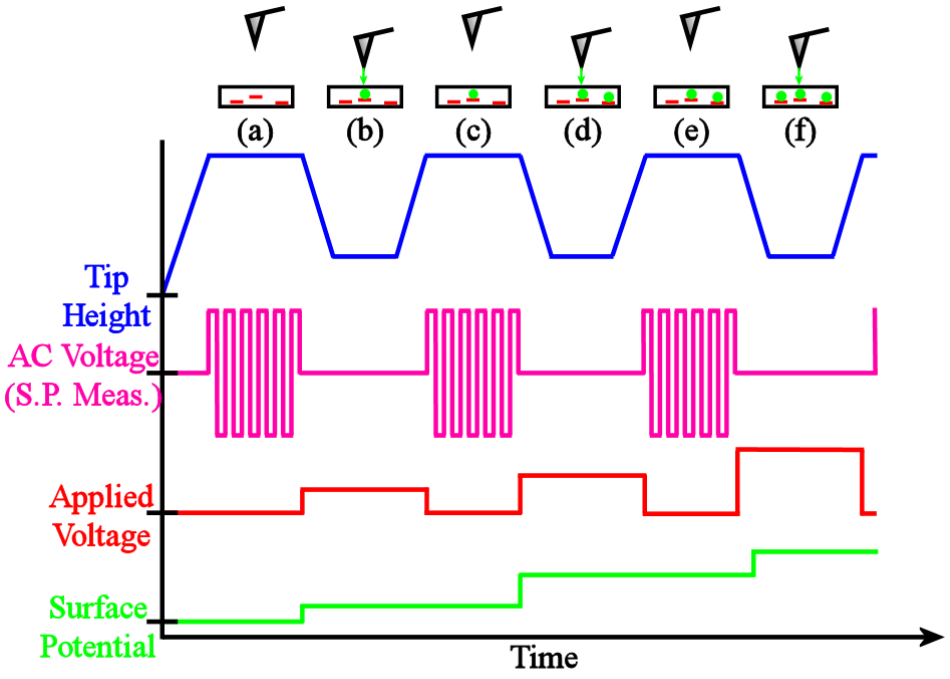

Figure 3.2: Diagram showing the applied voltages as a function of time. The energy spectrum of band gap states are probed by (a) increasing the sample/tip gap to 5.4 nm and turning on an AC square wave to measure the surface potential. (b) AC square wave is turned off, DC voltage is applied to the tip to induce tunneling. The tip/sample gap is reduced to 0.8 nm (tunneling range). The tip is stationary for a dwell time of 30 ms then is moved out to 5.4 nm and the DC voltage is turned off. (c) The surface potential is measured and the cycle is repeated with increasing applied voltages (d-f).

$$V_{gap} = \frac{z}{z + \frac{t_1}{k_1} + \frac{t_2}{k_2}} V_{App} \tag{3.1}$$

where z is the minimum tunneling gap, t_1 and t_2 are the thicknesses of the SiO_2 and HfO_2 films, respectively, k_1 and k_2 are the dielectric constants of the SiO_2 and HfO_2 films, respectively, and V_{APP} is the voltage applied to the sample with respect to the voltage that establishes the flatband condition. Under the sample conditions described above, an applied voltage of +10 V (-10 V) creates a tip-surface gap voltage difference of +5.95 V (-5.95 V), which places the tip Fermi-level above (below) the conduction (valence) mobility edges.

To determine if a parallel plate model is a reasonable model to calculate the voltage dropped in the gap, it was compared to a sphere-plate capacitor model[23]. With a 30 nm radius of curvature of the tip, a maximum error of 2% between the parallel plate model and that of the sphere-plate model was found when tunneling occurs within a 1 nm radius of the tip apex. Since the states that are being probed are of subnanometer dimensions,[24] the parallel plate model is sufficient.

SETFS measurements were taken at 40 locations on the HfO_2 sample. The relative apparent density of states is found for each applied voltage by differentially subtracting the surface potential values before and after each tunneling attempt. The results are plotted in Figure 3.3. Six representative apparent density of states traces, three above and three below flatband, each obtained at a different location, are shown. Note that the error at each point in the individual spectrum is smaller than the data points shown.

The six traces in Figure 3.3 (chosen as representatives of a set of forty measurements) show some similarities. All of the traces above mid-gap show a sharp rise in the apparent density of states at about 2.0 eV. There is an identifiable broad peak, below mid-gap, between -1.5 eV and -2.7 eV, which appears in all measurements made at all locations. There are also identifiable differences between each representative apparent density of states trace. Above mid-gap there is a small shoulder at about +1 eV (squares) that appears in only 1/3 of the measurement locations. This shoulder is not apparent in the literature, and may be due to surface states that are not

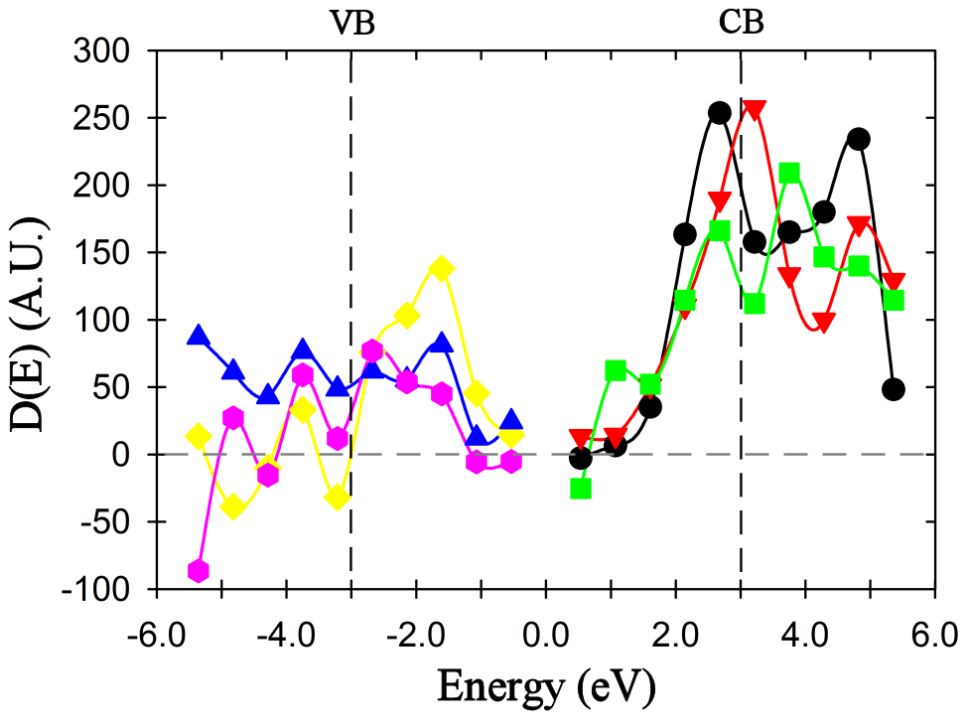

Figure 3.3: Representative plots of the apparent density of trap states within the band gap of HfO_2. The vertical, dotted line at -3 eV represents the valence band, while the one at +3 eV represents the conduction band.

detectable by traditional techniques. Although the traces below mid-gap all contain the broad peak, the peak has a significantly different shape for each trace. The difference in the apparent density of states traces for data taken at different locations is due to the inhomogeneous spatial distribution of defect states in the film.

The complete set of 40 measurements is averaged to compare with traditional techniques that measure the average apparent density of trap states (Figure 3.4). The average apparent density of trap states has a broad peak, which has a maximum at about +2.7 eV (0.3 eV below the conduction band). This peak corresponds well with the trap state measured by I-V curves,[4] charge pumping[5] and spectroscopic ellipsometry[25] at this energy. This state has also been theoretically predicted by Xiong *et al.*[26]

The broadening of the +2.7 eV peak is most likely due to the variation in physical depth of defect states in this energy range. In the apparent density of states data, the energy spectrum has been scaled using the voltage dropped between the tip and the trap. Since the depth of the states is unknown, an assumption is made that the trap states are at the sample surface, which does not take into account the additional voltage dropped in the oxide (between the sample surface and the deeper states). This causes such states to "appear" with an energy closer to the middle of the gap. In future measurements, this broadening can be eliminated using a recently demonstrated method, which provides for an independent determination of both the depth and energy of the states measured.[27] The presence of the lower apparent density peak (1/3 of the locations) at +1 eV may also cause broadening of the shoulder of the 2.7 eV peak in Figure 3.3.

Below mid-gap a broad peak from -1.5 eV to -2.7 eV is apparent. This broad peak may be associated with oxygen interstitial states, predicted by Xiong *et al.*[26] to be within 1 eV of the HfO_2 valence band. One of these states, a π^* state has been identified experimentally via electron spin resonance by Kang *et al.*[28]

In summary the apparent density of states in HfO_2 has been measured by Single Electron Tunneling Force Spectroscopy. The spectrum obtained by averaging spectra

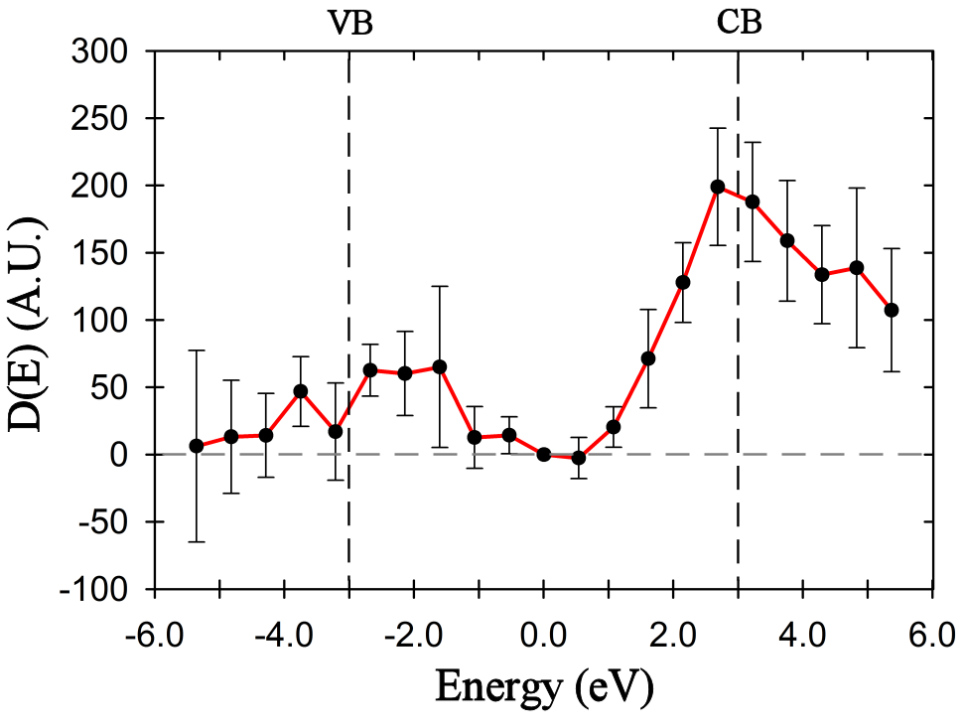

Figure 3.4: Apparent density of HfO_2 trap states averaged over 40 measurements locations. Of note is the peak at about +2.7 eV and the broad peak that spans from about -1.5 eV to -2.7 eV.

from many different locations shows a clear peak approximately 0.3 eV below the conduction band, which corresponds nicely with a defect state measured by standard I-V, charge pumping and spectroscopic ellipsometry methods. A broad peak from -1.5 eV to -2.7 eV has been identified and is in agreement with theory. The SETFS technique is sensitive to low density trap states, is able to measure states on completely nonconducting films, and provides information on trap state energy with nanometer scale spatial resolution.

The authors would like to thank the Semiconductor Research Corporation and IBM for funding this work and M. Frank and S. Zafar of IBM, T.J. Watson Research Center, for helpful discussions and for providing the HfO_2 samples.

3.2 References

[1] J. Robertson, Rep. Prog. Phys., 69, 327 (2006)

[2] G. Bersuker, J. H. Sim, C. S. Park, C. D. Young, S. V. Nadkarni, R. Choi, and B. H. Lee, IEEE Transactions on Device and Materials Reliability 7, 1, Pg 138 (2007)

[3] C. D. Young, Y. Zhao, D. Heh, R. Choi, B. H. Lee, and G. Bersuker, IEEE Transactions on Electron Devices 56, 6, Pg 1322 (2009)

[4] G. Ribes, S. Bruyère, D. Roy, C. Parthasarthy, M. Müller, M. Denais, V. Huard, T. Skotnicki, and G. Ghibaudo, IEEE Transactions on Device and Materials Reliability 6, 2, Pg. 132 (2006)

[5] A. Kerber and E. A. Cartier, IEEE Transactions on Device and Materials Reliability 9, 2, Pg 147 (2009)

[6] M. Placidi, A. Constant, A. Fontserè, E. Pausas, I. Cortes, Y. Cordier, N. Mestres, R. Pérez, M. Zabala, J. Millán, P. Godignon, and A. Pérez-Tomás, Journal of The Electrochemical Society, 157, 11, H1008-H1013 (2010)

[7] E. E. Hoppe and C. R. Aita, Appl. Phys. Lett. 92, 141912 (2008)

[8] J. W. Park, D. K. Lee, D. Lim, H. Lee, and S. H. Choi, J. Appl. Phys. 104, 033521 (2008)

[9] J. Price, P. S. Lysaght, S. C. Song, H. J. Li and A. C. Diebold, Appl. Phys. Lett. 91, 061925 (2007)

[10] N. V. Nguyen, A. V. Davydov, D. Chandler-Horowitz and M. M. Frank , Appl. Phys. Lett. 87, 192903 (2005)

[11] Q. Cai, Y. F. Hu, S. T. Hu, and X. Wang, J. Vac. Sci. Technol B 18, 5, Pg. 2384 (2000)

[12] H. Watanabe, Toshio Baba and M. Ichikawa , J. Appl. Phys. 87, 1 (2000)

[13] N. Miyata and M. Ichikawa, Phys. Rev. B 70, 073306 (2004)

[14] H. F. Cheng, Y. C. Lee, S. J. Lin, Y. P. Chou, T. T. Chen and I. N. Lin, J. Appl. Phys. 97, 044312 (2005)

[15] R. Stomp, Y. Miyahara, S. Schaer, Q. Sun, H. Guo, P. Grutter, S. Studenikin, P. Poole, and A. Sachrajda, Phys. Rev. Lett. 94, 056802 (2005)

[16] A. Dana and Y. Yamamoto, Nanotechnology 16, S125–S133 (2005)

[17] N. Zheng, J. P. Johnson, C. C. Williams and G. Wang, Nanotechnology 21, 295708 (2010)

[18] E. Bussmann and C. C. Williams, Appl. Phys. Lett. 88, 263108 (2006)

[19] E. Bussmann, Dong Jun Kim, and C. C. Williams, Appl. Phys. Lett. 85, 2538 (2004)

[20] E. Bussmann, N. Zheng and C. C. Williams, Nano Lett. 6, 2577 (2006)

[21] D.E. Eastman, Phys. Rev. B 2, 1 (1970)

[22] S. Monaghan, P. K. Hurley, K. Cherkaoui, M. A. Negara, and A. Schenk, Sol. St. Electron. 53, 438 (2009).

[23] F. F. Dall'Agnol, V. P. Mammana, Revista Brasileira de Ensino de Fisica 31, 3, 3503 (2009)

[24] J. P. Johnson, N. Zheng, and C. C. Williams, NanoTechnology 20, 055701 (2009)

[25] D. H. Hill, R. A. Bartynski,_N. V. Nguyen, A. C. Davydov, D. Chandler-Horowitz, and M. M. Frank, J. Appl. Phys. 103, 093712 (2008)

[26] K. Xiong, J. Robertson, M. C. Gibson and S. J. Clark, Appl. Phys. Lett 87, 183505 (2005)

[27] J. P. Johnson, D. W. Winslow and C. C. Williams, Appl. Phys. Lett. 98, 052902 (2011)

[28] A. Y. Kang, P. M. Lenahan and J. F. Conley, Jr., Appl. Phys. Lett. 83, 16, 3407 (2003)

CHAPTER 4

REVERSIBLE AND IRREVERSIBLE CHARGING OF HAFNIUM OXIDE FILMS

4.1 Abstract

The role of electron trap states in solid state memory devices has become more important in recent decades. To further the understanding of these defect states with atomic scale spatial resolution, single electron tunneling force spectroscopy has been developed and used to probe the charging behavior of electron trap states in HfO_2 films on a nanometer scale. Evidence of reversible and irreversible electron tunneling behavior is apparent in states both above and below the middle of the HfO_2 band gap. Evidence of irreversible charging of the HfO_2 trap states will be discussed and compared to the literature. A possible mechanism is proposed to explain the behavior of the charge in the dielectric film.

4.2 Introduction

The increased use of solid state drives as primary information storage devices and the use of high-K dielectrics[1] in electronic devices has motivated the study of electronic trap states. These defect states can cause undesirable behavior in solid state electronic devices through a reduction in carrier mobility in the channel, shifting of threshold voltage and an increase in leakage current.[2] Single Electron Tunneling Force Spectroscopy (SETFS) is well suited as a technique to study the behavior of charge in these trap states, because of its ability to inject and extract charge into electron traps in completely nonconducting films with atomic scale spatial resolution.[3, 4, 5, 6, 7, 8] In this study, SETFS is used to fill or empty electron trap

states in the HfO_2 band gap, and incrementally observe charge relaxation occurring in the films.

4.3 Method

Single Electron Tunneling Force Spectroscopy (SETFS)[3, 4, 6] is based on force detected single electron tunneling.[9, 10] It was developed to characterize individual, electrically isolated electron trap states with nanometer scale spatial resolution. Single electron tunneling occurs between a metalized AFM tip and these trap states. As the voltage between the AFM probe tip and the sample is varied, electrons are able to elastically tunnel into (and out of) trap states in the dielectric film. The tunneling events to states near or at the dielectric surface create an additional force gradient on the tip, shifting the resonant frequency of the AFM cantilever, and enabling detection of the tunneling events.[3] The change in surface potential is proportional to the number of electrons added to or removed from the trap states by tunneling.

The samples characterized in this study are 3.2 nm HfO_2 films grown on a 1.5 nm SiO_2 film on a Si substrate. Before the measurement, the samples were treated with a rapid thermal anneal at 1000 °C for 5 seconds. The SETFS measurements are obtained at room temperature in vacuum (~10^{-9} Torr) using an Omicron Multiprobe S Atomic Force Microscope (AFM) system. Each sample is prepared by ultrasonic wash and rinsed in acetone and isopropyl alcohol, after which the sample is rinsed with de-ionized water and blown dry with nitrogen. Once in the UHV chamber the sample is heated to 350 °C for 45 minutes to drive off any organic material on the sample surface. After the sample is cooled to room temperature, under vacuum, the AFM tip is moved to a height of 5.4 nm above the sample surface and an AC square wave (3 V_{peak} at ~ 300 Hz) is applied to measure the surface potential of the sample.[3, 4, 6] A DC offset voltage applied to the sample is adjusted until the flat band condition is reached (tip potential equal to surface potential). Once this condition is achieved the AC square wave is turned off and the system is ready to start the spectroscopic measurements.

A graphical representation of the waveforms used during the spectroscopic method can be seen in Figure 4.1. Figure 4.2 shows a toy model representing the occupation of the trap states during the different portions of the spectroscopic measurement. With the tip at a height of 5.4 nm with respect to the sample surface, the AC square wave is applied to measure the initial surface potential and is then turned off. A DC tunneling voltage (injection voltage) is applied to the sample to induce tunneling of electrons from the tip to the sample, and the tip/sample gap is reduced to 0.8 nm (tunneling range). If an empty trap state exists in the dielectric film, at or below the Fermi-level of the tip, an electron will elastically tunnel from the tip to the sample (Figure 4.2a). After a 30 ms tunneling attempt time, the tip is retracted (5.4 nm, out of tunneling range) and the DC voltage is turned off. The AC square wave is again applied between the tip and sample to measure the surface potential. After the surface potential is measured the AC square wave is turned off and a second DC tunneling voltage is applied, which has a smaller magnitude than the injection voltage previously applied. The tip is again moved within tunneling range of the sample (0.8 nm). During this tunneling attempt, electrons in states with energy between the first energy and the second energy will be extracted, by tunneling back to the AFM tip (Figure 4.2c). After this attempt (partial extraction) to extract charge in this energy range the tip is moved back out of tunneling range and the DC voltage is turned off. The AC square wave is again applied and the surface potential is measured. Next a DC voltage of 0.0 V_{App} is applied to the sample with respect to the applied flat band voltage and the tip is brought into contact with the sample surface with height feedback turned on. This step serves two purposes, the first being that it re-establishes the tip height with respect to the sample surface, which zeros height drift that has occurred during the measurement. Second, it should clear the surface of any injected electrons that have remained after the partial extraction tunneling attempt, and leave the sample ready for the next injection measurement. This last tunneling attempt will be referred to the reset attempt, because it is intended to reset the state occupation back to its condition before the injection and partial extraction

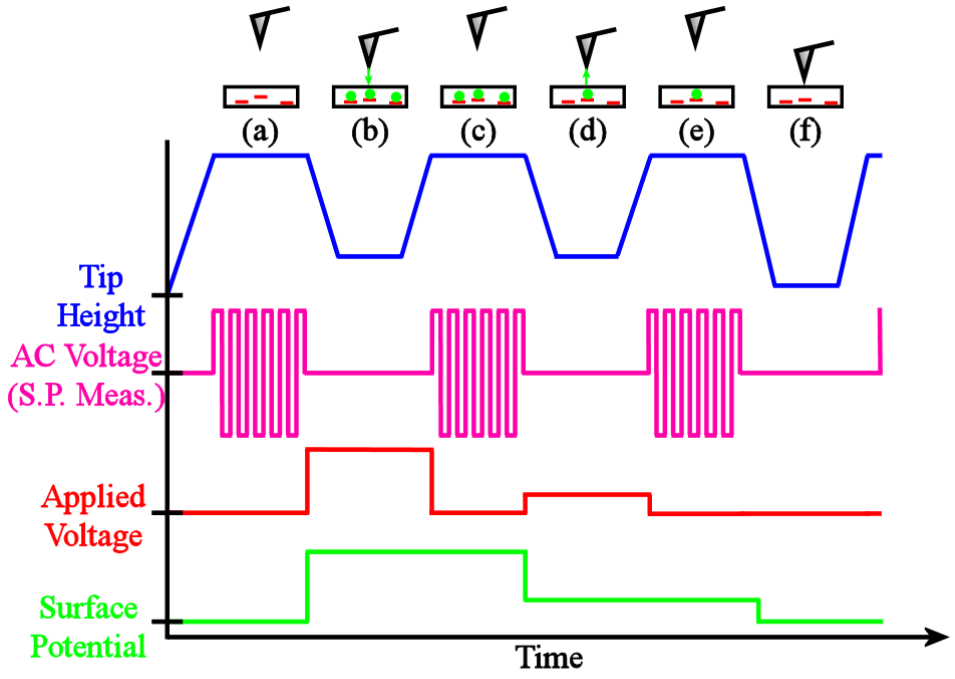

Figure 4.1: Graphical representation of a single measurement cycle. (a) The initial surface potential is measured, (b) Injection DC voltage is applied and the tip is moved within tunneling range of the sample, (c) tip moved out, DC is turned off and the surface potential is measured. (d) Partial extraction DC voltage applied and some of the injected electrons tunnel back to the tip. (e) Surface potential is measured, then the tip is brought into contact with 0 V DC applied with respect to flat band to clear any extracted charge and reset tip height.

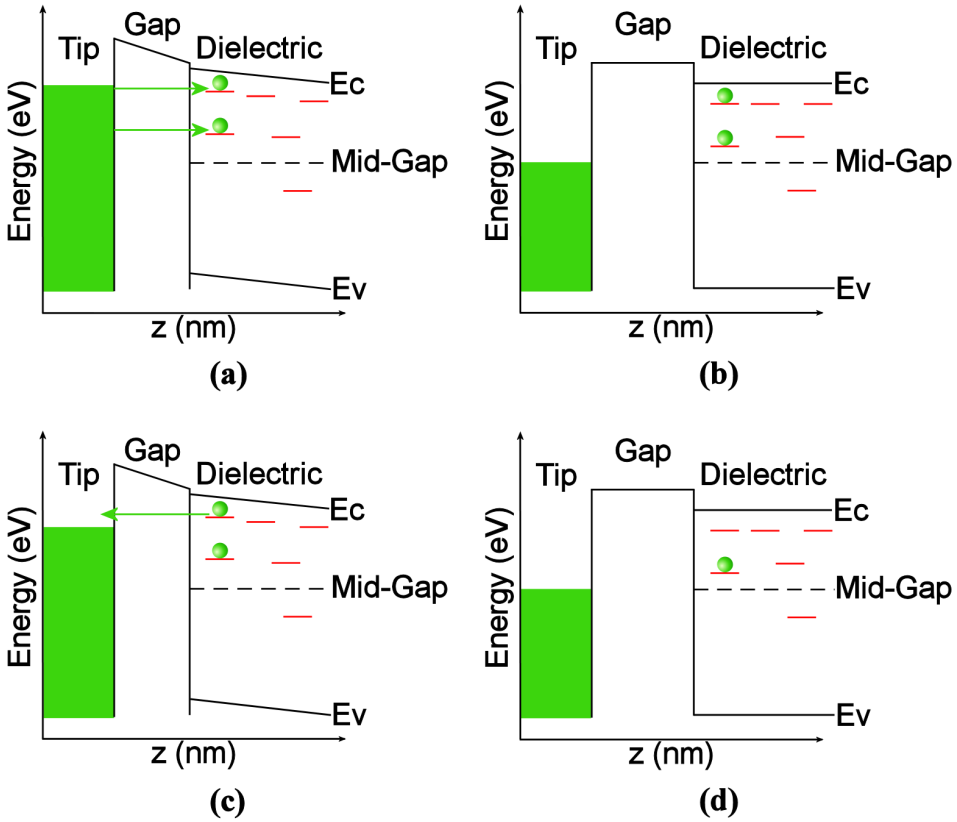

Figure 4.2: Graphical representation showing the tip-gap-sample system during the relaxation experiment. (a) A positive DC voltage is applied to the sample and electrons are able to elastically tunnel to the previously unoccupied trap states. (b) The gap is increased the DC voltage is turned off and the surface potential is measured. (c) A voltage lower than the voltage applied in part (a), but greater than 0 V is applied. Any electrons occupying trap states between the applied voltages in (a) and (c) will tunnel back to the tip from the trap states. (d) The DC voltage is turned off, the gap is increased and the surface potential is measured.

tunneling attempts were made. To probe the entire band gap this cycle is executed repeatedly for varying values of the applied injection voltages and applied partial extraction voltages. For the measurements discussed herein the applied injection voltages ranged between 1.0 V_{App} and 5.0 V_{App} (-1.0 V_{App}, -5.0 V_{App}), in increments of 1 V_{App}, while the applied partial extraction voltages ranged between 0.0 V_{App} with respect to the the flat band voltage and 1.0 V_{App} closer to the middle of the band gap than the previous applied injection voltage. For further clarity Figure 4.3 shows an example of the voltage array used to probe the relaxation of charge injected with an applied injection voltage of 4 V. The array has three separate voltages, the injection voltages represented by an "I", the partial extraction voltages represented by a "PE" and a reset voltage, which is equal to the initial flat band voltage, and is represented by an "R". It should be noted that for voltages below the middle of the band gap the initial applied voltage extracts (extraction attempt) electrons from the HfO_2 trap states and the subsequent applied voltage attempts to inject (partial injection attempt) these extracted electrons back into the unfilled states.

To establish the proper energy scale for these measurements the applied voltage must be scaled to the voltage dropped across the tip/sample gap. In this study a one dimensional parallel plate model is used to accomplish this, which has been shown to approximate the tip/sample system well.[7] In the case of the sample in this study an applied voltage of 5 V (-5 V) produces a gap voltage of approximately 2.8 V (-2.8 V), which allows the entire band gap of the HfO_2 to be probed.

4.4 Results and Discussion

Figure 4.4 shows a charge relaxation spectra for HfO_2 above the middle of the band gap taken at a single position on the sample surface. The red dashed line represents the surface potential after an injection attempt has been made, the blue dotted line is the surface potential after the partial extraction attempt and the black line is the surface potential measured after the tip has been placed on the surface with 0.0 V applied (reset attempt). It should be noted that each vertical bin in Figure 4.4

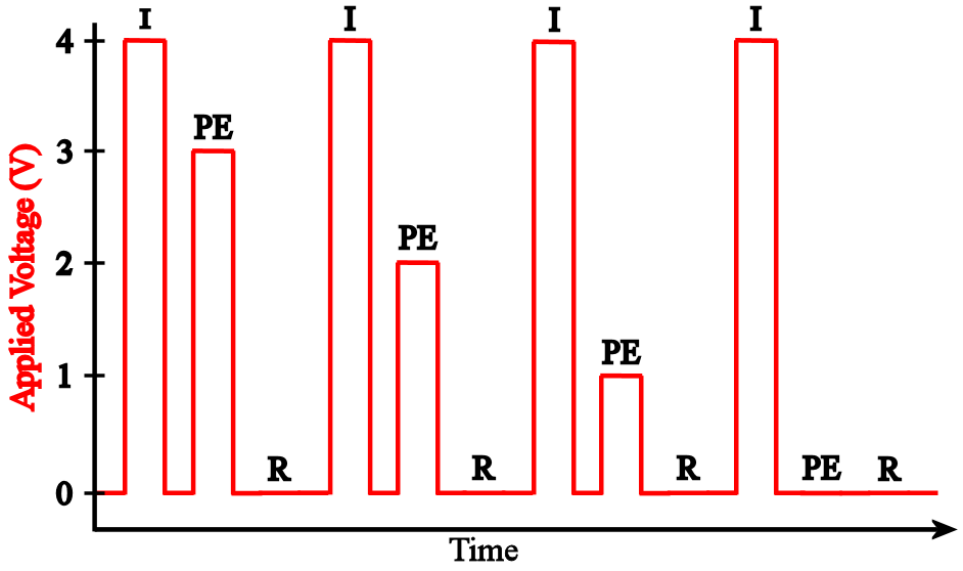

Figure 4.3: A representation of a voltage array used to probe the relaxation of charge in HfO_2. I represents the applied injection voltage (in this case 4 V), "PE" represents the applied partial extraction voltage and "R" represents the reset voltage, which is equal to the initial flat band voltage. This array is repeated with the same "I" and an incrementally reduced "PE" until an array with a "PE" equal to the flat band voltage is applied. It should be noted that a surface potential measurement is made between each labeled applied voltage, as per the explanation in Figure 4.1.

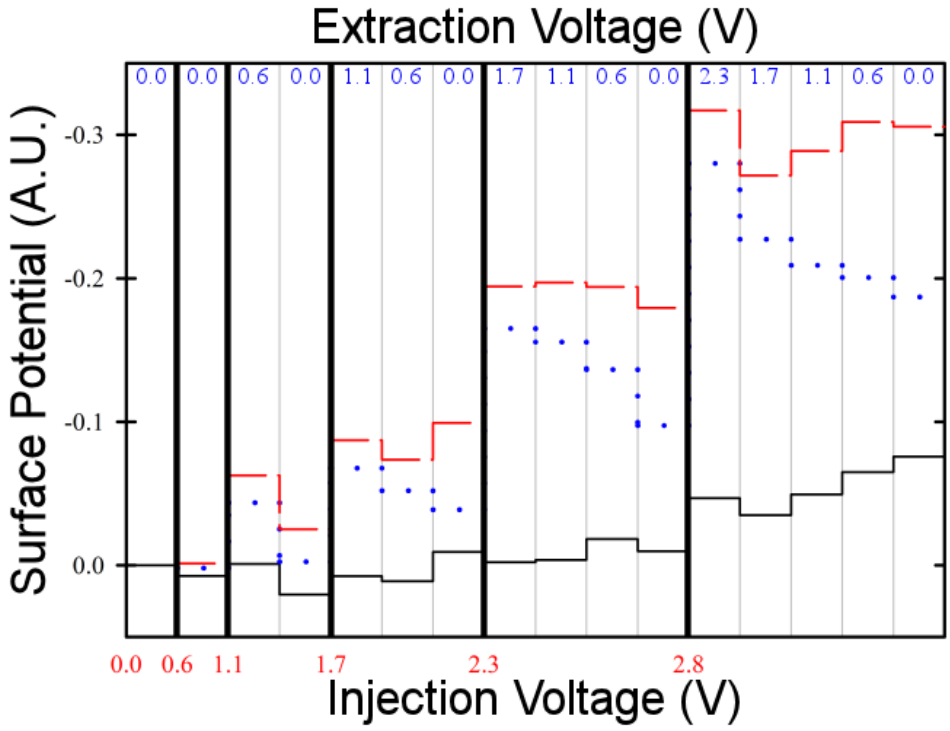

Figure 4.4: Surface potential measurements on HfO_2 above the middle of the band gap. The red dashed line is the surface potential after electron injection, the blue dotted line is after a partial extraction attempt and the black line is the surface potential after a reset attempt. The bottom horizontal axis shows the scaled injection voltage for each group of bins between the dark vertical lines. The blue numbers at the top of the graph indicate the partial extraction voltage for the bin.

represents a single set of injection (red dashed line), partial extraction (blue dotted line) and reset attempts (black). The difference between the red dashed and the blue dotted surface potential curves is proportional to the amount of charge that was extracted from trap states in the dielectric during the partial extraction attempt (blue numbers at the top of each bin). The difference between the blue dotted curve and the black curve is proportional to the amount of charge that was not extracted after the partial extraction attempt. Ideally all of the charge that is injected at a particular injection voltage should be completely extracted after a partial extraction attempt of 0.0 V, which would produce a completely flat black curve. However, as can be seen from Figure 4.4, this ideal case is not observed, indicating that a portion of the tunneled charge is remaining in trap states at the surface after the partial extraction and reset attempts. The red curve shows that at an injection voltage of 2.3 V twice the amount of charge was injected compared to the amount that tunneled to the surface at an injection voltage of 1.7 V. However, with an injection voltage of 2.3 V not all of the injected charge can be extracted from the dielectric material , even when an extraction tunneling voltage of 0.0 V is used only about one half of the total injected charge is extracted. This trend continues with an injection voltage of 2.8 V. In this case only about one third of the charge can be fully extracted. It should also be noted that, in addition to the irreversible surface charging discussed above, the reset voltage can not extract all of the trapped electrons after the 2.8 V injection attempt. The onset of the irreversible surface charging at a 2.3 eV injection is near the energy of a well established electron trap state at 2.7 eV, which is just below the HfO_2 conduction band, which has been measured by experiment[7, 11, 12, 13] and predicted theoretically.[14] This 2.7 eV state provides a possible tunneling path for the injected charge.

Figure 4.5 is representative of charge relaxation measurements made at a different location on the sample below the middle of the band gap. For the measurements made below the middle of the band gap the red dashed curve represents the surface potential after extraction, the blue dotted curve represents the surface potential after the

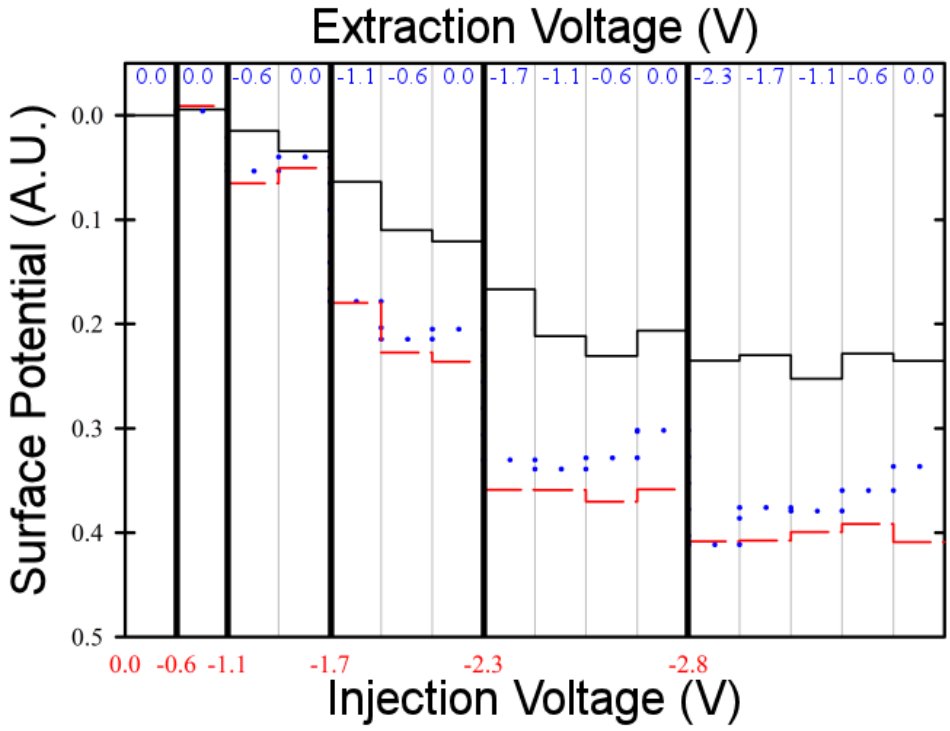

Figure 4.5: Surface potential measurements on HfO_2 below the middle of the band gap. The red dashed line is the surface potential after electron extraction, the blue dotted line is after a partial extraction attempt and the black line is the surface potential after a reset attempt. The bottom horizontal axis shows the scaled extraction voltage for each group of bins between the dark horizontal lines. The blue numbers at the top of the graph indicate the partial injection voltage for the bin.

partial injection attempt and the black is again the surface potential after the reset attempt. Below the middle of the band gap the irreversible surface charging is obvious starting with the -1.7 V extraction attempt. After the subsequent partial injection attempt of 0.0 V there is little difference between the red dashed (extraction) and blue dotted (partial injection) surface potential measurements. This very noticeable amount of irreversible surface charging is apparent throughout the larger extraction voltages. Also, unlike the measurements made above the middle of the band gap, the surface potential after the reset attempt shows an immediate inability to refill traps states that have been previously unloaded during the extraction attempt. The turn on of the irreversible surface charging behavior at -1.7 V corresponds with defect states measured in HfO_2[7] and predicted from theory.[14] This predicted π^* state is paramagnetic and has been shown to exist by ESR measurements.[15]

The irreversible nature of the surface charging, both above and below the middle of the band gap at greater extraction/injection voltages, may be due to the well known defect states discussed previously. Bersuker *et al.*[16] has posited that electrons that have tunneled into localized trap states, near the conduction band, in the HfO_2 band gap can relax away from the initially occupied state through adjacent trap states by Frenkel-Poole tunneling. Empirical evidence of this proposed mechanism was confirmed by measurement as one of several de-trapping mechanisms for electrons injected into HfO_2 by Heh *et al.*[17] Figure 4.6 diagrams a possible pathway that electrons may take through existing trap states. Initially the electron tunnels from the tip into an electron trap near the conduction band. After the injection attempt is made the electron is able to hop away from the surface of the sample through adjacent states near the conduction band. When the partial extraction attempt is made the electron is no longer within tunneling range of the tip and can not be extracted, but its presence can still be detected by the surface potential measurement. The SETFS relaxation measurements show an onset of charge relaxation just below the states known to be 0.3 eV below the HfO_2 conduction band (2.7 eV above middle of the band gap). This is corroborated by the temperature instability current

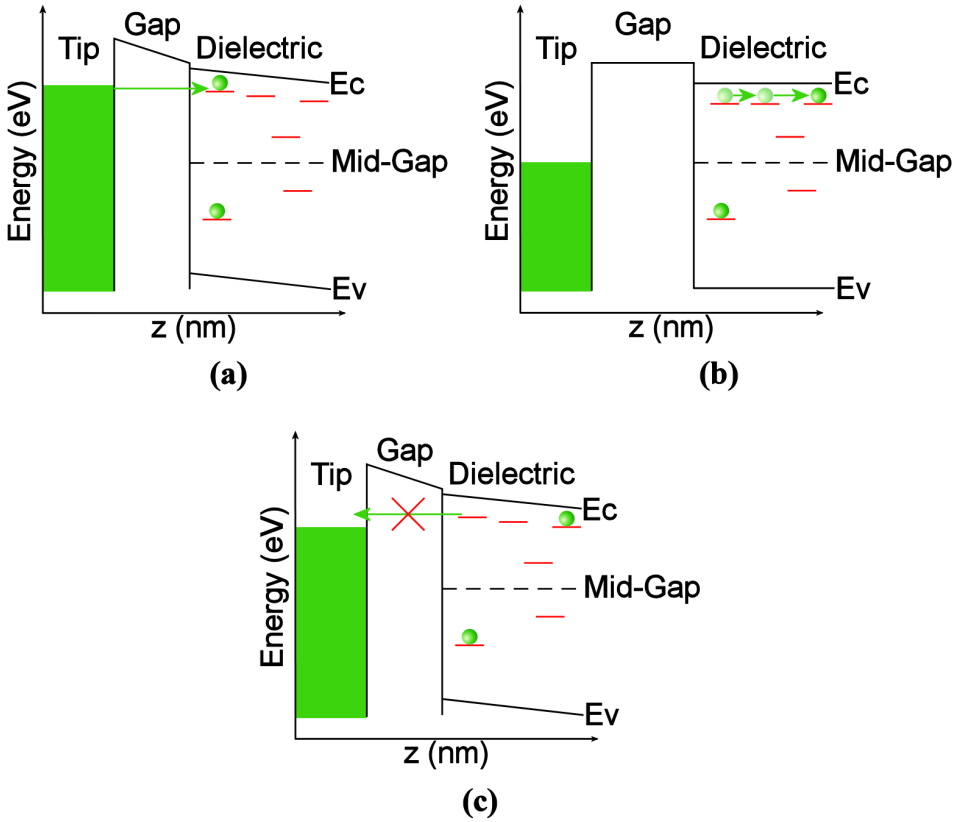

Figure 4.6: Description of possible pathway for mobile charge in HfO_2. Part (a) shows an electron tunneling into a trap state gap near the conducting band. (b) The electron is able to hop away from the surface of the HfO_2 through other nearby states. (c) The electron can not be extracted from the surface, because it is out of tunneling range of the tip, although its presence is still measured during the surface potential measurement.

voltage measurements made by Heh *et al.* The SETFS measurements were made at room temperature and show evidence of electron mobility just below the conduction band. However Heh *et al.* found evidence of the Frenkel-Poole tunneling only at operating temperatures of 125 ^{o}C. This may indicate that charge hopping is present at room temperature, but the current may be below the detectable level for the I_d-V_g measurements made by Heh *et al.* at room temperature. No evidence of mobile charge just above the HfO_2 valence band has been found in the literature. Since charge relaxation can be seen in Figure 4.5 this may be the first evidence of a similar charge hopping taking place below the middle of the HfO_2 band gap.

4.5 Conclusion

Single electron tunneling force spectroscopy has been used to show the behavior of electrons in trap states in HfO_2 films. Both irreversible and reversible charging is apparent, with the irreversible surface charging being more prevalent below the middle of the band gap than above, and more irreversible surface charging apparent near the conduction and valence bands than near the middle of the band gap. The evidence lends credence to the theory of charge relaxation put forth by Bersuker *et al.* for defect states near the HfO_2 conduction band. Additionally evidence has been found for electron hopping behavior of electrons in trap states below the middle of the band gap, which has not been found in the literature.

4.6 References

[1] J. Robertson, Rep. Prog. Phys. 69,327 (2006)

[2] G. D. Wilk, R. M. Wallace and J. M. Anthony, J. Appl. Phys. 89, 5243 (2001)

[3] E. Bussmann and C. C. Williams, APL, 88, 263108 (2006)

[4] E. Bussmann, N. Zheng and C. C. Williams Nano Lett. 6 2577 (2006)

[5] J. P. Johnson, N. Zheng and C. C. Williams, Nanotechnology 20, 055701 (2009)

[6] N. Zheng, J. P. Johnson, C. C. Williams and G. Wang, Nanotechnology, 21, 295708 (2010)

[7] D. W. Winslow, J.P. Johnson, and C. C. Williams, Appl. Phys. Lett. 98 172903 (2011)

[8] D. W. Winslow, C. C. Williams, J. of Appl. Phys. 110, 114102 (2011)

[9] L. J. Klein and C. C. Williams, J. Appl. Phys. 96, 3328 (2004)

[10] E. Bussmann, Dong Jun Kim, and C. C. Williams, Appl. Phys. Lett. 85, 2538 (2004)

[11] G. Ribes, S. Bruyère, D. Roy, C. Parthasarthy, M. Müller, M. Denais, V. Huard, T. Skotnicki, and G. Ghibaudo, IEEE Trans. Device Mater. Reliab. 6, 132 (2006)

[12] D. H. Hill, R. A. Bartynski, N. V. Nguyen, A. C. Davydov, D. Chandler-Horowitz, and M. M. Frank, J. Appl. Phys. 103, 093712 (2008)

[13] A. Kerber and E. A. Cartier, IEEE Trans. Device Mater. Reliab. 9, 147 (2009)

[14] K. Xiong, J. Robertson, M. C. Gibson, and S. J. Clark, Appl. Phys. Lett. 87, 183505 (2005)

[15] A. Y. Kang, P. M. Lenahan, and J. F. Conley, Jr., Appl. Phys. Lett. 83, 3407 (2003)

[16] G. Bersuker, J. H. Sim, C. S. Park, C. D. Young, S. V. Nadkarni, R. Choi and B. H. Lee, IEEE Transactions on Device and Materials Reliability, Vol. 7, No. 1, Mar 2007

[17] D. Heh, C. D. Young and G. Bersuker, IEEE Electron Device Letters, Vol. 29, No. 2, Feb. 2008

CHAPTER 5

CREATION OF DEFECT STATES IN SILICON DIOXIDE FILMS USING ELECTRON STIMULATED DESORPTION

5.1 Motivation and Objectives

The techniques developed in the Williams group and discussed thus far have been concerned with changing the occupancy of trap states,[1] imaging trap states,[2, 3] and spectroscopically probing the energy of trap states.[4, 5, 6, 7, 8] It naturally follows that one may want to know the chemical identity of the trap state being studied. To this end a single spin electron spin resonance (ESR) technique is under development in the Williams lab, in conjunction with the Boehme group at the University of Utah. The particulars of the proposed single spin ESR methodology will not be discussed in detail here, but the proposed methodology necessitates a paramagnetic trap state at the sample surface as well as at the apex of an AFM tip covered by a dielectric layer, unlike the previous techniques which used a metalized AFM tip.[9] The trap state that will be used in the preliminary measurements will be E' centers[10, 11] because of their long spin flip time (T_1) at room temperatures.[12] To achieve reliable and repeatable single spin ESR measurements, it is imperative that a method is developed that can reliably place a trap state at the apex of a SiO_2 coated atomic force microscope (AFM) tip. If trap states cannot be reliably located at the apex of the SiO_2 coated tip it will be difficult to consistently reproduce the paramagnetic state to state tunneling necessary to employ the single spin ESR measurement being developed.

There are several ways to produce E' centers in SiO_2 including bombarding the

sample with gamma rays,[13] photo-chemical techniques,[14] and plasma etching.[15, 16] However these techniques generally produce a spatially random distribution of trap states and do not allow the position of created traps to be precisely controlled. A method that has been used to produce single dangling bonds on the surface of hydrogen terminated Si is electron stimulated desorption (ESD).[17, 18, 19, 20, 21] ESD of hydrogen from a hydrogen terminated silicon surface is accomplished by bringing a scanning tunneling microscope (STM) probe to within a few nanometers of the H-terminated Si surface and applying a bias voltage between the tip and the sample surface. The hydrogen desorption is accomplished in one of two ways. If the voltage applied to the sample, with respect to the tip, is greater than 6 V, the electrons facilitating the desorption are typically field emitted from the tip.[17] These hot electrons can cause a bond state transition from the σ(Si-H) to the $^*\sigma$(Si-H) state.[17, 18] This excitation/desorption mechanism requires a large number of electrons and has a spatial injection accuracy of approximately ~ 5 nm when trying to control the position of the desorption on the surface. The second method occurs by tunneling electrons through the bond, which vibrationally excites the Si-H bond causing it to break.[17] The second method occurs between 2 eV and 5 eV and the place of desorption can be precisely controlled with atomic scale precision.[17, 18, 19, 20, 21]

The possibility is that if the ESD method can also be applied to an SiO_2 surface to remove the oxygen in an Si-O bond it could similarly create an E' center (also known as a dangling bond when referring to a defect at the surface) with atomic scale resolution. While the state could eventually be created at the apex of the SiO_2 coated AFM tip, this chapter will discuss first efforts to create the E' centers on a planar SiO_2 film.

5.2 ESD Methodology

The ESD attempts were made on a 10 nm SiO_2 film grown on a P-type Si substrate. The sample was cleaned by ultrasonic wash and rinse, first in acetone,

then isopropyl alcohol, after which the samples were rinsed with de-ionized water and blown dry with N_2. The samples were then loaded into the AFM chamber under ultra high vacuum (UHV ~ 10^{-9} Torr), and heated at 400 °C for 45 minutes. The sample was then placed in the AFM microscope and the tip is brought within 1 nm of the sample surface. A bias offset voltage was applied to bring the tip and sample into the flat band condition (no electric field in the vacuum gap).

In this experiment the ESD is being used on SiO_2, therefore some further considerations need to be made. During ESD on Si most of the voltage is dropped across the vacuum gap between the STM tip and the Si sample, except for the relatively small amount that is being dropped in the semiconductor. In the case of the SiO_2 film being used, it is beneficial to model the vacuum gap - oxide - Si system as two parallel plate capacitors in series. This model allows for a simple equation to calculate the portion of the voltage dropped between the AFM tip and the SiO_2 surface.

$$V_{gap} = \frac{z}{z + \frac{t}{k}} V_{App} \tag{5.1}$$

where z is the tip sample gap, t is the thickness of the SiO_2 film, k is the dielectric constant of the SiO_2, V_{App} is the voltage applied to the sample relative to the flat band voltage and V_{gap} is the voltage dropped between the tip and the oxide surface. This voltage also determines where the Fermi level of the tip is relative to the middle of the band gap at the surface of the dielectric.[1, 5] During these measurements the tunneling gap is 0.8 nm, the dielectric constant of SiO_2 is 3.9 and the thickness of the sample is 10 nm. These parameters produce a V_{gap} of approximately one fourth of V_{App}, which, along with the the 9 eV band gap of SiO_2, means that the voltages applied to the sample will need to be much greater than those used for ESD on silicon.

To show that a trap state could be created by the local ESD technique, a 30 nm by 30 nm surface topography measurement is taken to find a clear area of the oxide film surface. Then SETFM height scans[1] are performed in several places within a

small region of the surface, to find a location which does not have any df steps and therefore no available trap states to tunnel to. More specifically a bias voltage is applied to the sample with respect to the metalized AFM probe, and the probe is moved toward the surface. The frequency shift (df) of the oscillating cantilever is recorded as a function of the cantilever height from the sample surface. If there is an empty trap state at the surface an electron will tunnel from the tip to the trap state, which will cause an abrupt shift in the frequency of the cantilever oscillation, measured as a change in the df signal from the FM demodulator. This df step is evidence of an existent trap state (see Figure 5.1).

After a location with no state is found, the tip is moved to a height of approximately 0.8 nm from the surface and a positive voltage pulse is applied to the sample surface. After the voltage pulse, another SETFM height scan is performed to see if any new states are created by the voltage pulse. Any state created is identified by the new presence of a df step in the height scans (frequency shift versus height signal). Finally another topography scan is taken to ensure that no change in the surface morphology has occurred due to the applied voltage pulse. During the ESD attempts the size of the voltage pulse and its duration are varied to find a combination that would create a state at the surface, without modifying the surface morphology or the tip through field evaporation of its platinum coating.[22]

The length of the voltage pulse used for ESD ranged from a few seconds to approximately 1 μs. The magnitude of the applied voltage pulse ranged from 0 V to 50 V. A voltage pulse larger than about 40 V caused field evaporation of the Pt coating from the tip of the cantilever, leaving the tip unusable for SETFM measurements, because the conductive layer of the tip had been removed. With pulse heights between 20 V and 40 V and pulse lengths of 2-3 seconds, the SiO_2 surface directly under the tip was observed to be modified, becoming a mound believed to be a Taylor Cone, which consists of glassy SiO_2.[23] When the applied pulse width was less than about 100 μs with an applied voltage up to 30 V, no obvious surface deformation was observed. It should be noted that due to the finite capacitance of

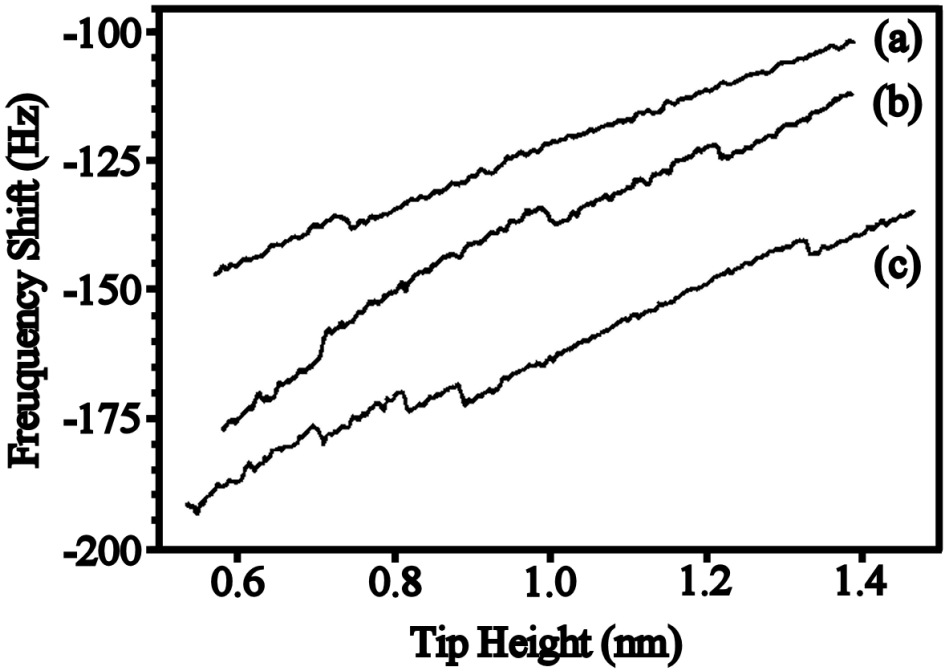

Figure 5.1: Three traces showing typical height curves showing the frequency shift steps indicative of single electron tunneling events. The data in these curves were taken by Ezra Bussman and are found in reference [1].

the AFM cables and hardware, any pulse shorter than about 50 μs did not appear as a sharp square pulse, but more closely resembled a triangular pulse. A pulse width of approximately 20 μs with a measured peak voltage of between 20 V and 23 V shows evidence of state production without changes in surface morphology.

5.3 Results and Discussion

Figure 5.2a shows a topographic scan of the surface taken before an applied voltage pulse of 21.5 V, while Figure 5.2b shows the same area of the surface after the voltage pulse. The voltage pulse was applied with the AFM tip in approximately the middle of the image. Note that there is no significant change in the surface morphology near the middle of the image. To further clarify the stability in the surface morphology during the measurement a difference image of Figures 5.2a and b can be seen in Figure 5.2c. Note that the size is somewhat smaller than the topographic images in both Figure 5.2a and b. This is because the lateral drift of the sample had to be compensated for when subtracting the images. Figure 5.3 shows two line cuts from Figures 5.2a and 5.2b, which were taken horizontally across each image approximately halfway down from the top of each image. The line cuts run across the area where the state creation attempt was made. Note that there is no evidence that the topography of the area has been significantly changed by the trap state creation attempt.

Figure 5.4 shows the SETFM height scans taken before and after the application of the 21.5 V pulse. The green curve (a) shows the SETFM height trace before the voltage pulse, the black curve (b) and the red curve (c) are representative of the SETFM height scans after the pulse was applied. The black SETFM curve (b) was taken immediately after the voltage pulse while the red curve (c) was taken, in the same spot, 15 to 20 seconds after the black. It should be noted that although the state creation attempt was made at the center of Figure 5.2, the location of the traces may be displaced from the center by approximately 1 nm due to the lateral drift of the tip with respect to the surface during the measurement. Frequency

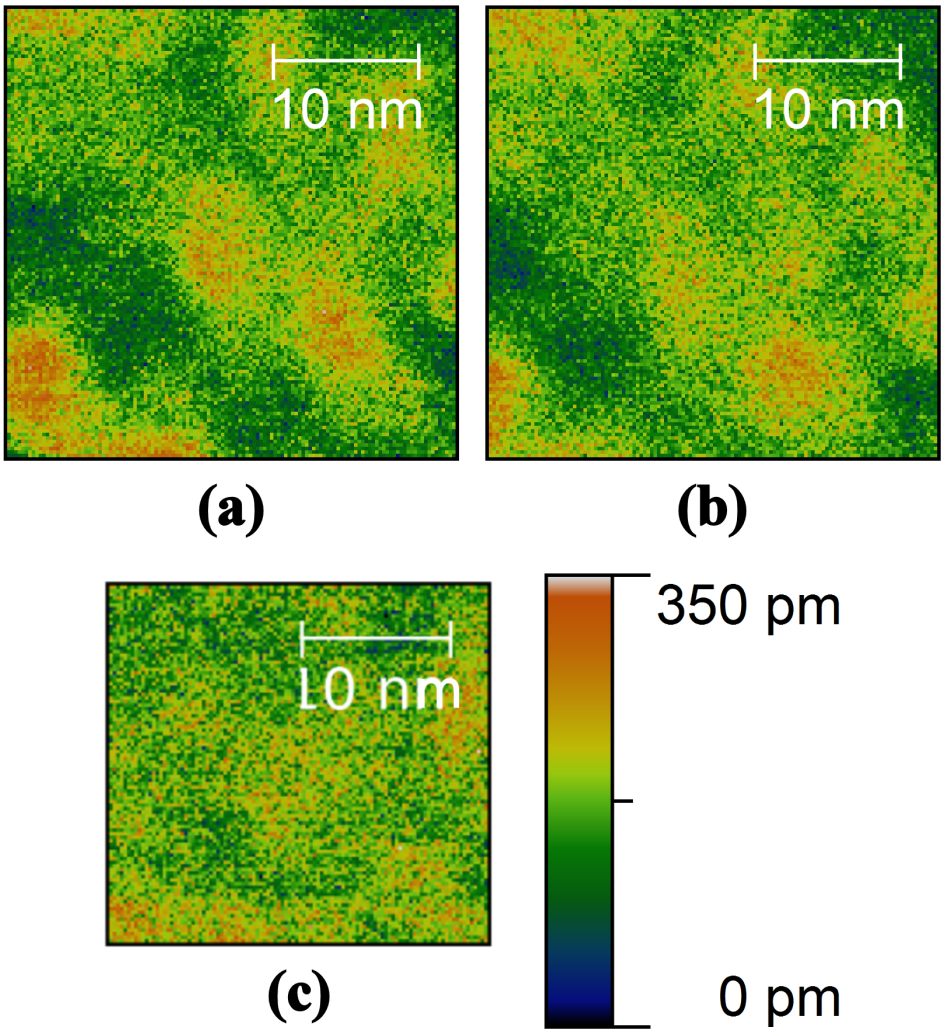

Figure 5.2: Comparison of surface topography before and after the state creation attempt. (a) A topographic image taken on the SiO_2 sample before a voltage pulse of 21.5 V is applied, while (b) is after the pulse has been applied. Notice that there is no major change in the surface morphology. (c) Difference image showing the stability of the surface under the ESD technique. The color scale next to (c) applied to all three images.

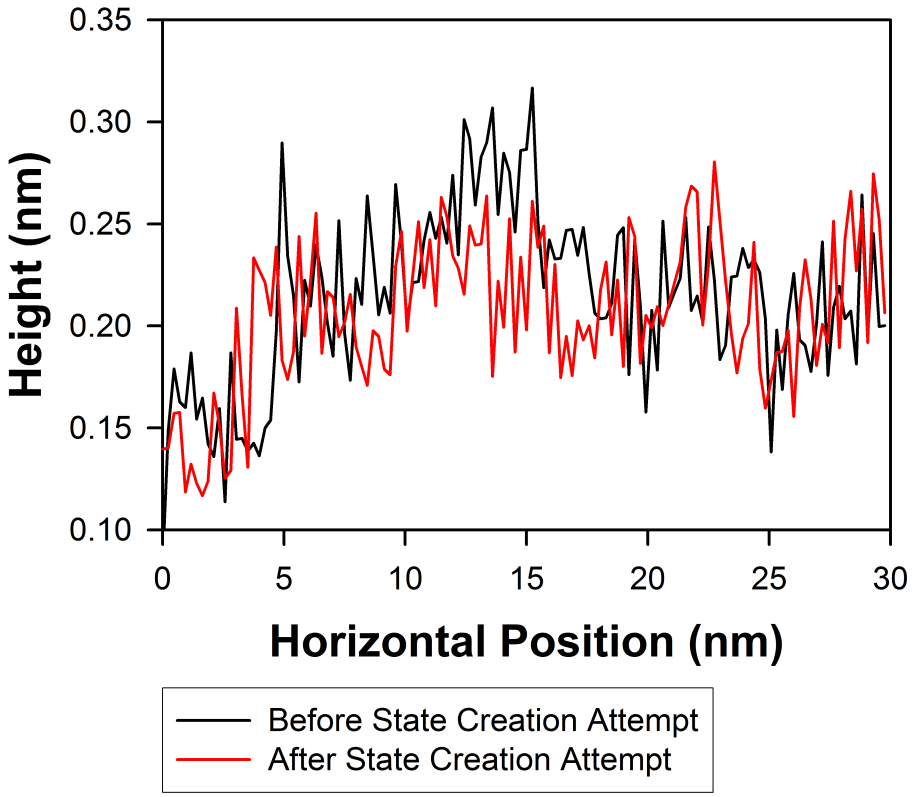

Figure 5.3: Line cuts taken horizontally across Figure 5.2a and 5.2b. Both curves run across the position where the state creation attempt was made. The black curve was taken on the topographic image measured before the state creation attempt (Figure 5.2a). The red curve was taken on the topographic image measured after the state creation attempt was made. Note that there is no significant change between the line cut taken before the state creation attempt and the one taken after the state creation attempt.

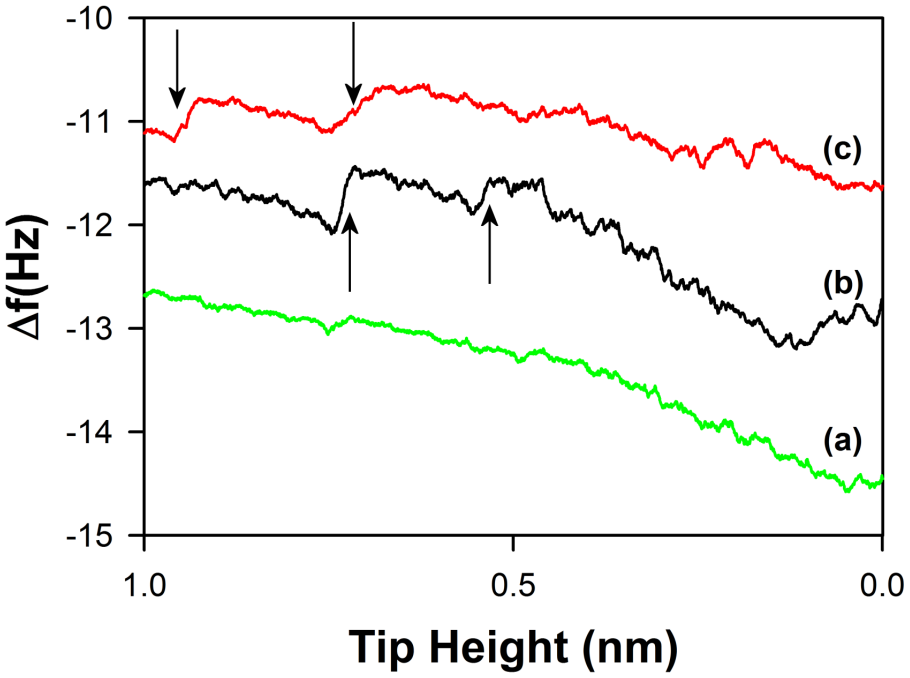

Figure 5.4: SETFM height scans taken on SiO_2 before (a) and after (b, c) a 21.5 V pulse applied 8 Å above the SiO_2 surface. Note the df steps in the after pulse traces signify the presence of trap states, which were not apparent during the height scan taken before the pulse. The (c) trace was taken approximately 20 seconds after the (b) trace.

shift changes of approximately 0.5 Hz indicate the presence of an electron that has tunneled between the tip and a state on the sample surface. There is an obvious change in the characteristics of the height scan curve before and after the application of the pulse. This is strong evidence that trap a state has been created under the tip by the attempted ESD pulse. The repeatability of the curves implies that the method may provide a means to generate the E' centers, needed to conduct the proposed single spin ESR measurements, in the film. However, further measurements must be made to be sure that the states created are E' centers. The reason the trap states do not occur in the same place in each scan is likely to the vertical and lateral drift of the tip with respect to the sample surface. Figure 5.5 shows traces taken at two separate locations on the surface after a 21.5 V pulse was applied. Attempted creation of trap states showed a success rate of about three in five attempts at this voltage.

The mechanism for the creation of the electron trap state may be similar to the mechanism posited for electron stimulated desorption of H off of an Si surface, which was discussed above. Although the SiO_2 surface used in this experiment was not hydrogen terminated any H terminated bonds would provide a ready place for state creation. Alternatively, the mechanism responsible for generating the defect states in the SiO_2 may be similar to a mechanism that causes device degradation in field effect transistor devices. In MOSFETS defects are created in both the Si channel and SiO_2 gate when hot electrons are injected into the MOSFET channel from the source electrode.[24, 25] The electrons with sufficient energy are able to enter the SiO_2 above the dielectric mobility edge, and create defects in the gate dielectric of the MOSFET device. These defects cause degradation of MOSFET functionally by creating a current path through the gate dielectric. However, the precise mechanism responsible for this reduction in functionality is still a topic of research. In the state creation attempts discussed above the voltage between the tip and the sample surface is sufficiently high to allow electrons to tunnel from the tip into states above the SiO_2 mobility edge. These relatively high energy electrons may be generating the

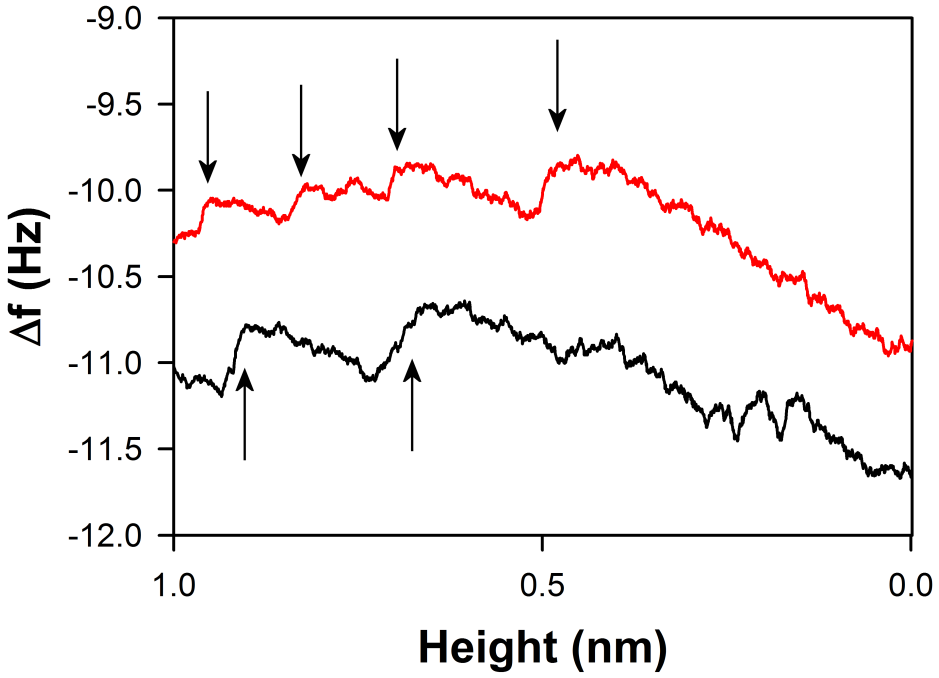

Figure 5.5: Two traces taken in two places after voltage pulses. Note the apparent existence of trap states in each trace, which are evident by df steps indicated with arrows. No states were apparent in the before state creation attempt traces for each of the traces above (not shown). There were no steps evident in the pre state creation attempt curves made before each curve in this figure.

same defects reported to cause degradation of MOSFET functionality or desorption of atoms at the SiO_2 surface.

5.4 Summary of ESD Results

Electron stimulated desorption has been attempted and conditions for ESD on SiO_2 have been studied. Evidence that trap states can be repeatably created near the oxide surface under controllable conditions has been shown. These preliminary results indicate that states can be created without significant modification of the sample surface topography. The traps created do not disappear after numerous SETFM height scans taken above the area at which the state creation attempt was made. However, if E' centers are the defects being created they should be stable under ultra high vacuum conditions. Although no specific mechanism for state creation has been identified, it has been posited that either atom desorption from the SiO_2 surface or a mechanism similar to that observed to cause MOSFET degradation may be the cause of the defect state creation. Further development of the technique and study of SiO_2 may provide for precise control of the trap state position in the oxide surface, and a better understanding of the state creation mechanism. The state creation technique discussed may also provide a means to create trap states (E' centers) at the apex of an oxidized AFM probe tip, needed for the proposed single spin ESR technique currently under development.

5.5 References

[1] E. Bussmann, D. Kim, and C. C. Williams, Appl. Phys. Lett. 85, 2538-2540 (2004)

[2] E. Bussmann, N. Zheng and C. C. Williams, Nano Letters 6, 2577-2580 (2006)

[3] J. P. Johnson,, N. Zheng and C. C. Williams, Nanotechnology 20, 055701 (2009)

[4] E. Bussmann, and C. C. Williams, Appl. Phys. Lett. 88, 263108 (2006)

[5] N. Zheng, J. P. Johnson, C. C. Williams and G. Wang, Nanotechnology 21, 295708 (2010)

[6] Johnson, J.P. and Winslow, D.W. and Williams, C.C., APL 98, 052902 (2011)

[7] Winslow, D.W. and Johnson, J.P. and Williams, C.C., APL 98, 172903 (2011)

[8] Winslow, D. W. and Williams, C. C. (accepted for publication), J. Appl. Phys.

[9] Johnson, J. P. Thesis, University of Utah

[10] O' Reilly, E. P. and Robertson, J., Phys. Rev. B, 27 (6) 1983

[11] Nicklaw, C. J., Lu, Z.-Y., Fleetwood, D. M., Schrimpf, R. D. and Pantelides, S. T., IEEE Transactions on Nuclear Science, 49 (6) 2002

[12] Ghim, B.T. and Eaton, S.S. and Eaton, G.R. and Quine, R.W. and Rinard, G.A. and Pfenninger, S., Journal of Magnetic Resonance, Series A, 115, 230-235 (1995)

[13] Zvanut, M. E., Stahlbush, R. E. and Carlos, W. E., APL 60, 24 (1992)

[14] Messina, F. and Cannas, M., J. Phys.: Condens. Matter 18, 9967-9973 (2006)

[15] Yokogawa, K., Yajima, Y., Mizutani, T., Nishimatsu, S. and Suzuki, K., Japanese J. of Appl. Phys. 29 (10), 2265-2268 (1990)

[16] Yokogawa, K., Yajima, Y., Mizutani, T., Nishimatsu, S. and Ninomiya, K., Japanese J. of Appl. Phys. 30 (11B), 3199-3202 (1991)

[17] Shen, T.-C. and Wang, C. and Abeln, G.C. and Tucker, J.R. and Lyding, J.W. and Avouris, Ph. and Walkup, R.E., Science 268, 1590-1592 (1995)

[18] Shen, T.-C. and Avouris, P., Surface Science 390, 35-44 (1997)

[19] Reusch, T.C.G. and Curson, N.J. and Schofield, S.R. and Hallam, T. and Simmons, M.Y., Surface Science 600, 318-324 (2006)

[20] Tong, X. and Wolkow, R.A., Surface Science 600, L199-L203 (2006)

[21] Haider, M.B. and Pitters, J.L. and Dilabio, G.A. and Livadaru, L. and Mutus, J.Y. and Wolkow, R.A., PRL 102 (2009)

[22] Koyanagi, H., Hosaka, S., Ryo Imura, R. and Shirai, M., Appl. Phys. Lett. 67 (18) 1995

[23] Staufer, U. and Wiesendanger, R. and Eng, L. and Rosenthaler, L. and Hidber, H.R. and Güntherodt, H.-J. and Garcia, N.

[24] S. Tam, P-K Ko and C. Hu, IEEE Transactions on Electron Devices ED-31, 9 (1984)

[25] D. J. DiMaria, J. Appl. Phys. 87, 12 (2000)

APPENDIX

COMPARISON OF TIP-GAP-SAMPLE CAPACITANCE MODELS

Chapter 1 discussed the need to find an adequate model to approximate the tip-gap-sample system. This appendix discusses two models proposed to approximate the system. The first, simpler model uses two parallel plate capacitors in series to model the tip-vacuum gap-dielectric substrate system (Figure A.1a). The second uses a spherical-plate capacitor model that is partially filled with the dielectric under consideration (Figure A.1b).

Under the parallel plate model the scaled voltage dropped in the gap is given by

$$V_{gap} = \frac{z}{z + \frac{t}{\epsilon}} V_{App} \tag{A.1}$$

where z is the tunneling gap, t is the thickness of the oxide, ϵ is the dielectric constant of the dielectric material, V_{App} is the voltage applied to the tip with respect to the grounded sample electrode and V_{gap} is the voltage dropped between the tip and the dielectric surface.[1] Note that for these two models the sample is grounded with respect to an applied voltage on the tip. This has been done for clarity of description. However, in the actual experiment the tip has been grounded and the voltage is applied to the sample. For a typical measurement condition the tunneling gap is 0.8 nm, the thickness of the dielectric is 10 nm and the dielectric constant of SiO_2 is 3.9. If the applied voltage is -1 V a V_{gap} of -0.24 V is achieved, which means that the surface of the dielectric is at a potential of -0.76 V. This means that if there is a trap state 0.24 eV above the middle of the SiO_2 band gap the energy condition will be met to allow tunneling from the metalized tip to the trap state in the dielectric.

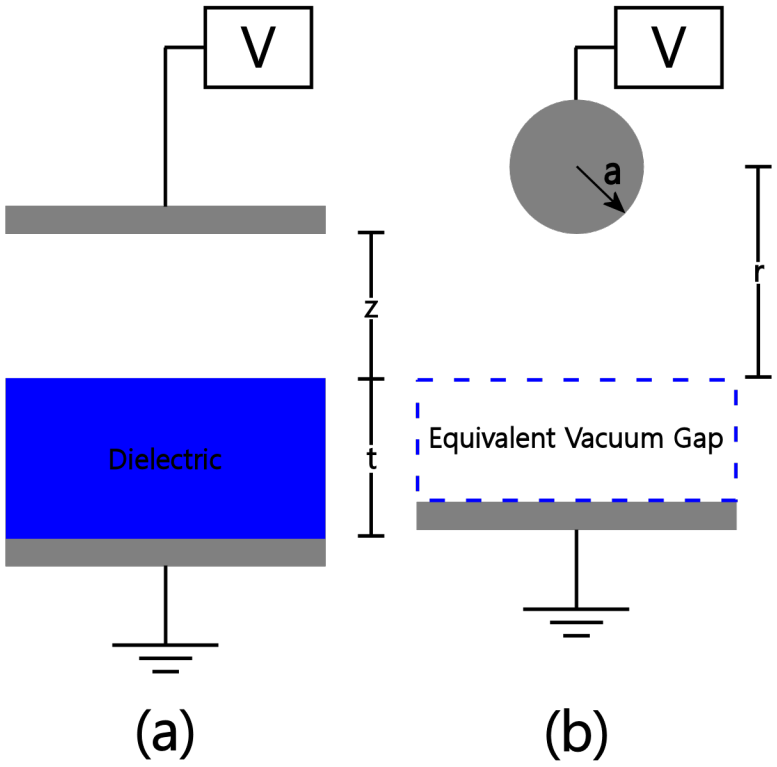

Figure A.1: Diagram showing the two capacitor models being compared. (a) shows a parallel plate model in which the tip (top electrode) has a voltage applied to it with respect to the grounded electrode attached to the dielectric. (b) shows the same set up, but the tip is now being approximated as a metallic sphere instead of a plate.

Under the sphere-plate capacitor model the potential in the gap is calculated by the method of images and is given by,[2]

$$V(z,r) = aV_{App}\sum_{i=0}^{\infty}\frac{\xi_i}{((z-z_i)^2+r^2)^{\frac{1}{2}}} - \frac{\xi_i}{((z+z_i)^2+r^2)^{\frac{1}{2}}} \tag{A.2}$$

with,

$$\xi_i = \frac{a}{z_0 + z_{i-1}}\xi_{i-1} \tag{A.3}$$

$$z_i = z_0 - \frac{a^2}{z_0 + z_{i-1}} \tag{A.4}$$

$$z_0 = a + z + \frac{t}{\epsilon} \tag{A.5}$$

where in equation A.2 a is the radius of the sphere, which is representing the tip in this model, r is the radial distance from the center of the sphere, and perpendicular to the plate surface, to the point where the electric potential is to be determined, z_i is the position of the ith image charge with respect to the plate surface, z_0 is given by the equation A.5, z is the height at which the voltage is to be determined with respect to the dielectric surface and ξ_i is the coefficient given by $\xi_i = \frac{q_i}{q_0}$, which is the ratio of the ith image charge and the charge on the sphere due to the applied voltage V. See Figure A.1b for a better understanding of the variables being used in the sphere-plate model. The coordinates used for the model are polar. The third term in equation A.5 is known as the effective vacuum gap of the dielectric. This is the distance of vacuum that would be needed to replace the dielectric and have a capacitance equivalent to the dielectric. If the experimental parameters from the parallel plate model are put in, including a tip radius of 30 nm which gives a z_0 of 33.4 nm, an applied voltage of -1 V gives a gap voltage of -0.25 V, which puts the potential at the dielectric surface at -0.75 V. This means that the percent difference between the parallel-plate model and the sphere-plate model is about 1.5%. Due to the minimum error incurred the parallel plate model is used to approximate the system.

A.1 References

[1] N. Zheng, J. P. Johnson, C. C. Williams and G. Wang,Nanotechnology 21, 295708 (2010)

[2] F. F. Dall'Agnol and V. P. Mammana, Revista Brasileira de Ensino de Fisica 31, 3503 (2009)